On the SNR Penalties of Ideal and Non-ideal Subset Diversity Systems

Wesley M. Gifford, *Member, IEEE*, Andrea Conti, *Senior Member, IEEE*, Marco Chiani, *Fellow, IEEE*, and Moe Z. Win, *Fellow, IEEE*

***Abstract*—Subset diversity (SSD) techniques, which select and combine the signals from a subset of the available diversity branches, are important for practical wireless systems. This paper characterizes the performance loss, or signal-to-noise ratio (SNR) penalty, of one SSD system with respect to another. Both ideal and non-ideal channel estimation are considered, and the analysis is valid for the important case of arbitrary two-dimensional signal constellations. Expressions are given for the asymptotic SNR penalty, for both small and large SNR, for all the comparisons considered. Additionally, we develop bounds and approximations to quantify the performance of one system in terms of another for all SNRs of interest. Furthermore, for some signal constellations, we derive the exact SNR penalty of a non-ideal system with respect to an ideal system, as well as the exact penalty associated with two non-ideal systems with varying degrees of estimation energy. The SNR penalty enables the assessment of system sensitivity to channel estimation energy, combining architecture, and signal constellation.**

***Index Terms*—Fading channels, non-ideal channel estimation, performance evaluation, signal-to-noise ratio penalty, subset diversity.**

I. Introduction

DIVERSITY techniques are essential for modern wireless systems as increasingly more demands are placed on their capabilities. While the performance of these systems increases with the number of utilized diversity branches, the complexity and resource consumption also increases. These issues have motivated the use of methods that process only a *subset* of the available diversity branches [1]–[10]. These subset diversity (SSD) systems, where only a subset of the signals on the available $N_{\rm d}$ diversity branches are selected and then combined, are capable of achieving full diversity [11]–[14]. SSD arises naturally as a generalization of other diversity methods which include selection diversity, where the best branch is selected, and hybrid selection/maximal-ratio combining (H-S/MRC), where the best $L_{\rm d}$ out of $N_{\rm d}$ diversity branches are selected [15]–[18]. The particular combining scheme defines the *combining architecture*, a term we will use to refer to which diversity branches are selected and utilized by a receiver.

SSD can be exploited in the spatial, temporal, frequency, angle, or polarization domains. In particular, one of the most popular applications of SSD is in the spatial domain, where the number of radio frequency chains is less than the number of antenna elements. In this case, only signals from a selected subset of antennas are processed. This is advantageous in terms of cost and energy consumption; consequently, transmit and receive antenna selection is included in several next-generation wireless standards. For example, standards such as IEEE 802.11n for WiFi [19], 3GPP for long-term evolution [20], [21], and IEEE 802.16 for WiMAX [22] specify schemes for antenna selection.

Many previous studies of SSD have assumed that perfect channel knowledge is available. For example, in [23], it was shown that ideal H-S/MRC achieves a diversity order equal to the number of available diversity branches, despite using only a subset of them. In the sense that these systems have perfect channel knowledge, they can be thought of as having the best possible *estimation accuracy*. However, practical diversity receivers must estimate the channel on each diversity branch and, thereby, incur a performance loss [24]–[36]. In the case of SSD, the estimation plays a dual role: it affects both the selection process as well as the combining mechanism. Thus, in SSD, it is possible that an erroneous selection is made, because the diversity branches chosen are based on an estimate of the channel.

When comparing diversity systems, differences in the combining architectures and estimation accuracies can cause a performance loss or a signal-to-noise ratio (SNR) penalty. In general, this loss occurs because completely coherent combining is not possible *and* because the selection mechanism is not perfect. Specifically, in ideal SSD systems the loss occurs due to the fact that only some of the diversity branches are utilized. In non-ideal SSD systems, the loss occurs because not only a subset of the branches is used, but also the selection and combining is based on imperfect channel estimates. A suitable measure of this loss is the SNR required to maintain a target symbol error probability (SEP) [23]. The SNR penalty is the increase in SNR required for one system to achieve the same target SEP as

Manuscript received October 16, 2009; revised October 31, 2010; accepted April 11, 2011. Date of current version May 15, 2012. This work was supported in part by the National Science Foundation under Grant ECCS-0901034, the Office of Naval Research Presidential Early Career Award for Scientists and Engineers (PECASE) N00014-09-1-0435, the Office of Naval Research under Grant N00014-11-1-0397, the MIT Institute for Soldier Nanotechnologies, the Italian Ministero dello Sviluppo Economico under the Project WEBS and by the European Concerto Project under Grant 288502.

W. M. Gifford was with the Laboratory for Information and Decision Systems, Massachusetts Institute of Technology, Cambridge, MA 02139 USA. He is now with the IBM Thomas J. Watson Research Center, Hawthorne, NY 10532 USA (e-mail: wgifford@ieee.org).

A. Conti is with ENDIF, University of Ferrara, Ferrara 44100, Italy and also with WiLAN, University of Bologna, Cesena 47521, Italy (e-mail: a.conti@ieee.org).

M. Chiani is with the DEIS, University of Bologna, Cesena 47521, Italy (e-mail: marco.chiani@unibo.it).

M. Z. Win is with the Laboratory for Information and Decision Systems, Massachusetts Institute of Technology, Cambridge, MA 02139 USA (e-mail: moewin@mit.edu).

Communicated by G. Taricco, Associate Editor for Communications.

Color versions of one or more of the figures in this paper are available online at http://ieeexplore.ieee.org.

Digital Object Identifier 10.1109/TIT.2011.2178131

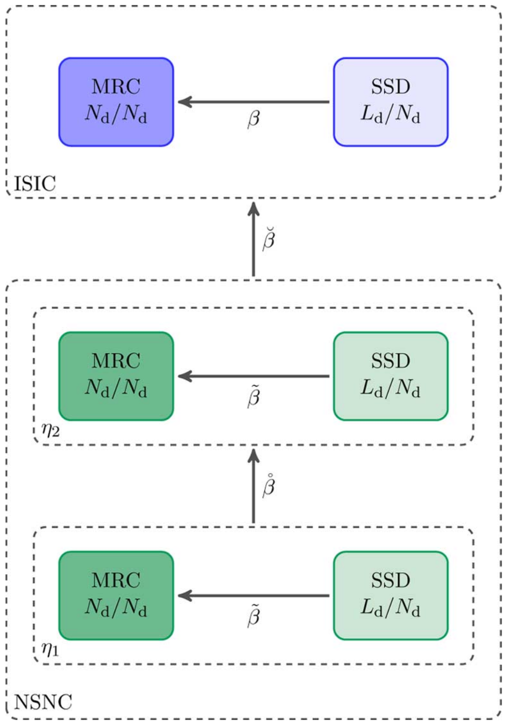

Fig. 1. Pictorial description of the considered system comparisons. For each comparison, the arrows point in the direction of the reference system.

a reference system. In general, the SNR penalty is a function of the target mean SEP (averaged over the small-scale fading) and, therefore, is also a function of the average SNR. Understanding the SNR penalty enables system designers to quickly approximate or bound the performance of one diversity system in terms of another. In [23], [37], [38], the asymptotic SNR penalties, for both small and large SNR, were considered for ideal H-S/MRC systems and different combining architectures.

This paper considers two classes of SSD systems with arbitrary two-dimensional signal constellations in Rayleigh fading. These two classes are ideal selection with ideal combining (ISIC) and non-ideal selection with non-ideal combining (NSNC). In the former system, the selection of diversity branches and the subsequent combining utilizes ideal (or perfect) channel estimates. In the latter system, both the selection and combining utilize non-ideal (or imperfect) channel estimates. We specifically consider four penalties that arise between these two classes of systems. These comparisons are illustrated pictorially in Fig. 1 and are described in detail in Section IV. For a given combining scheme using M-PSK signaling, we derive the exact SNR penalty of a non-ideal system with respect to an ideal system, as well as the exact penalty associated with two non-ideal systems with varying degrees of estimation accuracy. For arbitrary two-dimensional constellations, we derive the asymptotic expressions for the SNR penalties, for both small and large SNR. Then, we derive upper and lower bounds on the SNR penalty in a few cases. Finally, we obtain accurate approximations for all SNR penalties under consideration. In addition to these results, this paper unifies the results in [23], [37], and further extends the analysis to include the effects of non-ideal channel estimation.

The remainder of this paper is organized as follows. Section II gives the model for the systems under consideration. In Section III we provide the exact SEP expressions for both ISIC and NSNC systems and derive the asymptotic expressions. In Section IV we describe the SNR penalties on interest, and derive asymptotic expressions for a variety of comparisons. Bounds on the SNR penalties and useful approximations are given in Section V. Numerical results are discussed in Section VI, and finally, conclusions are given in Section VII.

II. Model

We consider a diversity system with N_d available antenna elements utilizing an arbitrary two-dimensional M-ary signal constellation with polygonal decision boundaries. The received signal on the $k\mathrm{th}$ diversity branch, after demodulation, matched filtering, and sampling, is given by

$$r_k = h_k s_m + n_k, \quad k = 1, 2, \ldots, N_\mathrm{d}$$

where s_m, $m = 1, 2, \ldots, M$, represents the complex message symbol, h_k is the complex, multiplicative channel gain on the $k\mathrm{th}$ branch, and n_k is a sample of additive noise on the $k\mathrm{th}$ branch. The average symbol energy is indicated by E_s. The additive noise is modeled as a circularly symmetric complex Gaussian random variable (RV) with zero mean and variance $N_0/2$ per dimension and is assumed to be independent among the diversity branches. We consider independent, identically distributed Rayleigh fading channels, i.e., each channel gain can be written as a circularly symmetric complex Gaussian RV, $h_k = h_{k,\mathrm{r}} + jh_{k,\mathrm{i}}$, with $\mathbb{E}\{h_k\} = 0$ and $\mathbb{E}\left\{|h_k|^2\right\} = \mathbb{E}\left\{|h_{k,\mathrm{r}}|^2\right\} + \mathbb{E}\left\{|h_{k,\mathrm{i}}|^2\right\} = 2\sigma_h^2$.

An ISIC system has knowledge of the true channel gains, $\boldsymbol{h} = [h_1\ h_2\ \cdots\ h_{N_\mathrm{d}}]$. In this case, the output of the SSD combiner is given by [11], [16], [17]

$$D = \sum_{k \in \mathcal{O}_\mathrm{I}} h_k^* r_k \tag{1}$$

where $\mathcal{O}_\mathrm{I}$ is a set of indices indicating which subset of diversity branches to combine. The indices contained in $\mathcal{O}_\mathrm{I}$ are determined from the ordered magnitudes of the channel gains through a binary-valued selection vector, $\boldsymbol{a}$. Note that since an ISIC SSD system operates with perfect channel knowledge, no errors are made during the selection and combining processes.

In practice, however, a system does not have direct access to $\boldsymbol{h}$. Instead the channel gains must be estimated; thus the combiner output is [26], [30], [34], [39], [40]

$$D = \sum_{k \in \mathcal{O}_\mathrm{N}} \hat{h}_k^* r_k \tag{2}$$

where $\mathcal{O}_\mathrm{N}$ indicates which branches to combine and $\hat{h}_k$ is the estimate of the channel gain, h_k. Clearly, the performance of this combining scheme greatly depends on the quality of the channel estimate $\hat{h}_k$. The indices contained in $\mathcal{O}_\mathrm{N}$ are determined from the ordered magnitudes of the *estimated* channel gains through a binary-valued selection vector, $\boldsymbol{a}$. Note that since the selection is based on the *estimated* magnitude of the channel gains, it is possible that an error is made during the selection process, i.e.,

$\mathcal{O}_{\mathrm{N}}$ is not necessarily equal to $\mathcal{O}_{\mathrm{I}}$. An estimate of the channel gains can be formed by averaging N_{p} pilot symbols, each with energy E_{p}, received within the coherence time of the channel.[1] In this case, the resulting estimate is[2]

$$\hat{h}_k = h_k + e_k$$

where e_k is the complex Gaussian estimation error with zero mean and variance $\sigma_e^2 = N_0/(2\varepsilon E_{\mathrm{s}} N_{\mathrm{p}})$ per dimension. The pilot energy is related to the signal energy through the quantity $\varepsilon = E_{\mathrm{p}}/E_{\mathrm{s}}$. Note that $\hat{h}_k$ is a complex Gaussian RV since it is the sum of two complex Gaussian RVs. It is important to stress that N_{p} represents the number of *received* pilot symbols used in forming an estimate of each branch. Depending on the choice of transmitter and receiver architectures of an SSD system, the actual number of transmitted pilots may need to be larger to guarantee an estimate of each branch based on N_{p} pilots.[3]

III. SEP OF ISIC AND NSNC SYSTEMS

In this section, we first review the exact SEP expressions for ISIC and NSNC systems. Using these results, we then derive expressions for the asymptotic SEP. Later, these expressions will play a critical role in deriving the SNR penalties.

A. Exact SEP Expressions

In [30], [42], it was shown that the SEP expressions for two-dimensional M-ary signal constellations have the same structure for ISIC and NSNC. The expressions differ only in the parameter $\zeta(\Gamma)$, which is a function of the average branch SNR, $\Gamma = 2\sigma_h^2 \frac{E_{\mathrm{s}}}{N_0}$. This structure is given by

$$P_{\mathrm{e}}(\Gamma) = \sum_{i=1}^{M} p_i \sum_{j \in \mathcal{B}_i} I_{N_{\mathrm{d}}}(\boldsymbol{\zeta}^{(i,j)}(\Gamma), \phi_{i,j}, \psi_{i,j}) \tag{3}$$

where p_i is the *a priori* probability that the *i*th symbol is transmitted and

$$I_{N_{\mathrm{d}}}(\boldsymbol{\zeta}(\Gamma), \phi, \psi) \triangleq\triangleq \frac{1}{2\pi} \int_0^{\phi} \prod_{n=1}^{N_{\mathrm{d}}} \left[\frac{\sin^2(\theta+\psi)}{\sin^2(\theta+\psi) + \zeta_n(\Gamma)} \right] d\theta. \tag{4}$$

In (3) $\mathcal{B}_i$ is the set of indices for the signaling points that share a decision boundary with s_i and the angles $\phi_{i,j}, \psi_{i,j}$ describe the decision region corresponding to s_i (see Fig. 2 for an example).[4] The SEP depends on Γ through the vector $\boldsymbol{\zeta}^{(i,j)}(\Gamma)$, whose elements depend on the particular signaling scheme, combining method, and channel estimation. The nth element of $\boldsymbol{\zeta}^{(i,j)}$ is given by

$$\zeta_n^{(i,j)}(\Gamma) = b_n \frac{w_{i,j}}{4} \Gamma \quad \text{(ISIC)} \tag{5}$$

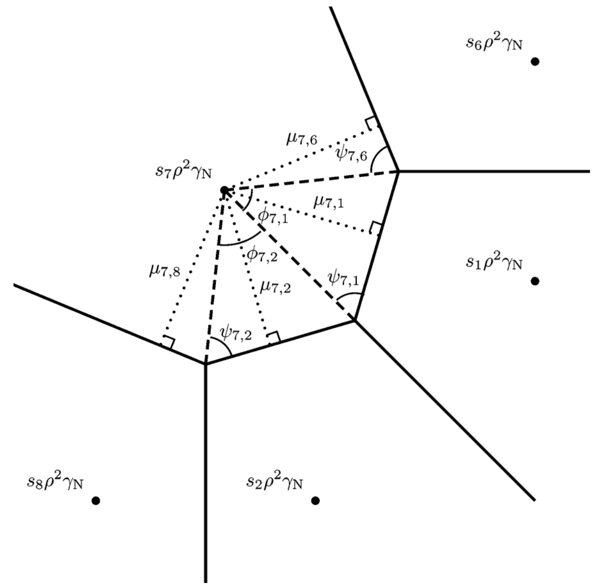

Fig. 2. Portion of the received signal constellation and its associated decision regions.

$$\zeta_n^{(i,j)}(\Gamma) = b_n \frac{w_{i,j}}{4} \frac{\eta\Gamma^2}{1+(\eta+\xi_i)\Gamma} \quad \text{(NSNC)} \tag{6}$$

where the quantity $w_{i,j}$ is related to the distance between s_i and s_j and is defined as $w_{i,j} = \xi_i + \xi_j - 2\sqrt{\xi_i\xi_j}\cos(\theta_i - \theta_j)$. The signal points are represented in polar form as $s_i = \sqrt{\xi_i E_{\mathrm{s}}} e^{j\theta_i}$ with $\xi_i \triangleq \frac{E_i}{E_{\mathrm{s}}}$. The term $\eta = N_{\mathrm{p}}\varepsilon$ represents the amount of energy devoted to channel estimation, normalized to the energy of one data symbol.

The quantity b_n is the nth element of $\boldsymbol{b} = \boldsymbol{T}_{\mathrm{VB}}^T \boldsymbol{a}$, and the lth element of $\boldsymbol{a}$, $a_l \in \{0, 1\}$, determines whether the diversity branch with the lth largest estimated magnitude is included in the combining process. The upper triangular virtual branch transformation matrix, $\boldsymbol{T}_{\mathrm{VB}} : \mathbb{R}^{N_{\mathrm{d}}} \to \mathbb{R}^{N_{\mathrm{d}}}$, is given by [12]

$$\boldsymbol{T}_{\mathrm{VB}} = \begin{bmatrix} 1 & \frac{1}{2} & \cdots & \frac{1}{N_{\mathrm{d}}} \\ & \frac{1}{2} & \cdots & \frac{1}{N_{\mathrm{d}}} \\ & & \ddots & \vdots \\ & & & \frac{1}{N_{\mathrm{d}}} \end{bmatrix}. \tag{7}$$

Note that for MRC $\boldsymbol{a} = \mathbf{1}$, yielding $\boldsymbol{b} = \mathbf{1}$, where $\mathbf{1}$ is a vector of 1s. In this case, ζ_n does not depend on n and we have

$$P_{\mathrm{e}}^{\mathrm{MRC}}(\Gamma) = \sum_{i=1}^{M} p_i \sum_{j \in \mathcal{B}_i} I_{N_{\mathrm{d}}}^{\mathrm{MRC}}(\boldsymbol{\zeta}^{(i,j)}(\Gamma), \phi_{i,j}, \psi_{i,j}) \tag{8}$$

where

$$I_{N_{\mathrm{d}}}^{\mathrm{MRC}}(\boldsymbol{\zeta}(\Gamma), \phi, \psi) \triangleq \frac{1}{2\pi} \int_0^{\phi} \left[\frac{\sin^2(\theta+\psi)}{\sin^2(\theta+\psi) + \zeta(\Gamma)} \right]^{N_{\mathrm{d}}} d\theta. \tag{9}$$

For certain signaling schemes, the SEP expressions can be further simplified. For M-PSK, due to the symmetry of the constellation, the SEP can be expressed as a single integral

$$P_{\mathrm{e}}^{M-\mathrm{PSK}}(\Gamma) = 2 I_{N_{\mathrm{d}}}\left(\boldsymbol{\zeta}(\Gamma), \frac{M-1}{M}\pi, 0\right) \tag{10}$$

[1]Note that the channel estimation process is carried out to track changes in the channel, and thus, pilot symbols need only be transmitted with a rate suitable to track the fading [41].

[2]In this case, the result is the maximum likelihood estimate [26].

[3]For example, in the case of antenna diversity with L_{d} receiver chains, if $L_{\mathrm{d}} < N_{\mathrm{d}}$ it is not possible to receive the transmitted pilots on all branches simultaneously. It can be shown that $\lceil N_{\mathrm{d}}/L_{\mathrm{d}} \rceil N_{\mathrm{p}}$ pilots need to be transmitted to ensure at least N_{p} pilots are received for estimation on each of the N_{d} branches.

[4]A detailed derivation of (3) and (4), along with the definitions of γ_{N}, ρ, and $\mu_{i,j}$ is available in [30].

where the expression for $\boldsymbol{\zeta}(\Gamma)$ uses $w_{i,j} = 4\sin^2(\pi/M)$. For M-QAM, the SEP can be expressed as a weighted sum of two integrals

$$P_{\mathrm{e}}^{M-\mathrm{QAM}}(\Gamma) = \frac{1}{M}\sum_i \omega_i^a I_{N_{\mathrm{d}}}\left(\boldsymbol{\zeta}^{(i)}(\Gamma), \frac{\pi}{2}, \frac{\pi}{4}\right) + \omega_i^{\mathrm{b}} I_{N_{\mathrm{d}}}\left(\boldsymbol{\zeta}^{(i)}(\Gamma), \frac{3\pi}{4}, 0\right) \quad (11)$$

where ω_i^a and ω_i^{b} are given in [30], and the expression for $\boldsymbol{\zeta}(\Gamma)$ uses $w_{i,j} = 12/[2(M-1)]$.

B. Asymptotic SEP Expressions

In this section, we derive the asymptotic behavior of the SEP for small and large SNR, as it will play a central role later in developing expressions for the asymptotic penalties of interest. The notation $P_{\mathrm{e;ISIC}}$ is used to denote (3) using the ISIC expression for $\zeta_n^{(i,j)}$ (5). Similarly, $P_{\mathrm{e;NSNC}}$ denotes (3) with the NSNC expression for $\zeta_n^{(i,j)}$ (6).[5]

Lemma 1: For asymptotically small Γ and finite η, the expansion of $P_{\mathrm{e;ISIC}}(\Gamma)$ and $P_{\mathrm{e;NSNC}}(\Gamma)$ is given, respectively, by[6]

$$P_{\mathrm{e;ISIC}}(\Gamma) \approx P_{\mathrm{e;a,ISIC}}(\Gamma)$$
$$P_{\mathrm{e;NSNC}}(\Gamma) \approx P_{\mathrm{e;a,NSNC}}(\Gamma)$$

where

$$P_{\mathrm{e;a,ISIC}}(\Gamma) \triangleq \frac{\bar{\phi}}{2\pi} - \frac{\bar{\omega}}{2}\kappa(\boldsymbol{b})\Gamma^{1/2} + o\left(\Gamma^{1/2}\right) \quad (12a)$$
$$P_{\mathrm{e;a,NSNC}}(\Gamma) \triangleq \frac{\bar{\phi}}{2\pi} - \eta^{1/2}\frac{\bar{\omega}}{2}\kappa(\boldsymbol{b})\Gamma + o(\Gamma) \quad (12b)$$

with

$$\kappa(\boldsymbol{b}) = \frac{1}{2\pi}\int_0^\infty \left\{1 - \prod_{n=1}^{N_{\mathrm{d}}}\left(\frac{u^2}{b_n + u^2}\right)\right\} du$$
$$\bar{\phi} = \sum_{i=1}^{M} p_i \sum_{j\in\mathcal{B}_i} \phi_{i,j}$$
$$\bar{\omega} = \sum_{i=1}^{M} p_i \sum_{j\in\mathcal{B}_i} w_{i,j}^{1/2}[\mathbb{1}_{\{\psi_{i,j}=0\}} + \mathbb{1}_{\{\psi_{i,j}+\phi_{i,j}=\pi\}}]$$

and $\mathbb{1}_B$ is an indicator function, defined as

$$\mathbb{1}_B = \begin{cases} 1, & \text{if } B \text{ is true} \\ 0, & \text{otherwise.} \end{cases} \quad (13)$$

Proof: To prove (12b), we will use Lemma 3 and Lemma 4 given in Appendix A. From (3), (4), and (6)

$$P_{\mathrm{e;NSNC}}(\Gamma) = \sum_{i=1}^{M} p_i \sum_{j\in\mathcal{B}_i} I_{i,j}(\Gamma;\phi_{i,j},\psi_{i,j}) \quad (14)$$

where

$$I_{i,j}(\Gamma;\phi_{i,j},\psi_{i,j}) \triangleq \frac{1}{2\pi}\int_{\psi_{i,j}}^{\phi_{i,j}+\psi_{i,j}} \prod_{n=1}^{N_{\mathrm{d}}}\left[\frac{\sin^2\theta}{b_n\frac{w_{i,j}}{4}\frac{\eta\Gamma^2}{1+(\eta+\xi_i)\Gamma} + \sin^2\theta}\right] d\theta. \quad (15)$$

Also note that, based on geometrical considerations, $\phi_{i,j} + \psi_{i,j} \leq \pi$. For each $I_{i,j}(\Gamma;\phi_{i,j},\psi_{i,j})$ term in the summation (14) there are several cases to consider:

1) $\psi_{i,j} > 0, \phi_{i,j} + \psi_{i,j} < \pi$: Application of Lemma 3 yields

$$I_{i,j}(\Gamma;\phi_{i,j},\psi_{i,j}) \approx \frac{\phi_{i,j}}{2\pi} + o(\Gamma). \quad (16)$$

2) $\psi_{i,j} = 0, \phi_{i,j} < \pi$: Application of Lemma 4 yields

$$I_{i,j}(\Gamma;\phi_{i,j},0) \approx \frac{\phi_{i,j}}{2\pi} - \left[\frac{\eta\omega_{i,j}}{4}\right]^{1/2}\kappa(\boldsymbol{b})\Gamma + o(\Gamma). \quad (17)$$

3) $\psi_{i,j} > 0, \phi_{i,j} + \psi_{i,j} = \pi$: In this case, using the symmetry of $\sin^2\theta$

$$\begin{aligned} I_{i,j}(\Gamma;\pi-\psi_{i,j},\psi_{i,j}) &= I_{i,j}(\Gamma;\pi-\psi_{i,j},0) \\ &= I_{i,j}(\Gamma;\phi_{i,j},0) \\ &\approx \frac{\phi_{i,j}}{2\pi} - \left[\frac{\eta\omega_{i,j}}{4}\right]^{1/2}\kappa(\boldsymbol{b})\Gamma + o(\Gamma) \end{aligned} \quad (18)$$

where the last equivalence follows from case 2.

4) $\psi_{i,j} = 0, \phi_{i,j} = \pi$: Using the symmetry of $\sin^2\theta$

$$\begin{aligned} I_{i,j}(\Gamma;\pi,0) &= 2I_{i,j}(\Gamma;\pi/2,0) \\ &\approx 2\frac{\pi}{4\pi} - 2\left[\frac{\eta\,\omega_{i,j}}{4}\right]^{1/2}\kappa(\boldsymbol{b})\Gamma + o(\Gamma) \\ &= \frac{\phi_{i,j}}{2\pi} - 2\left[\frac{\eta\,\omega_{i,j}}{4}\right]^{1/2}\kappa(\boldsymbol{b})\Gamma + o(\Gamma) \end{aligned} \quad (19)$$

where the second equivalence follows from case 2.

Using (16)–(19) in (14) completes the proof.

The proof of (12a) can be completed using similar steps as above in conjunction with [23, Lemma 1]. □

Note that the quantity $\bar{\omega}$ includes contributions from the triangular sub-decision regions of a particular signaling point where $\psi_{i,j} = 0$ or $\phi_{i,j} + \psi_{i,j} = \pi$. For this case, the sub-decision region must be located on the edge of the signal constellation. When the SNR is asymptotically small, the variance of the received signal increases with respect to the mean, making it likely that the received signal will cross a decision boundary and the receiver will make an error. The only place where a boundary cannot be crossed is at the edge of the constellation. The second term in (12a) and (12b) quantifies this probability.

Lemma 2: For asymptotically large Γ, the expansion of $P_{\mathrm{e;ISIC}}(\Gamma)$ and $P_{\mathrm{e;NSNC}}(\Gamma)$ is given, respectively, by

$$P_{\mathrm{e;ISIC}}(\Gamma) \approx P_{\mathrm{e;A,ISIC}}(\Gamma)$$
$$P_{\mathrm{e;NSNC}}(\Gamma) \approx P_{\mathrm{e;A,NSNC}}(\Gamma)$$

[5]Throughout the paper, the subscript "*a*" is used to denote expressions that are applicable for asymptotically small SNR, while the subscript "*A*" is used to denote expressions that are applicable for asymptotically large SNR.

[6]A function $f(x) \in o(g(x))$ if and only if $\lim_{x\to 0}\frac{f(x)}{g(x)} = 0$.

where

$$P_{\mathrm{e;A,ISIC}}(\Gamma) \triangleq \frac{1}{\Gamma^{N_\mathrm{d}}}\left(\prod_{n=1}^{N_\mathrm{d}}\frac{1}{b_n}\right)\sum_{i=1}^{M}p_i I_i + o\left(\frac{1}{\Gamma^{N_\mathrm{d}}}\right) \quad (20a)$$

$$P_{\mathrm{e;A,NSNC}}(\Gamma) \triangleq \frac{1}{\Gamma^{N_\mathrm{d}}}\left(\prod_{n=1}^{N_\mathrm{d}}\frac{1}{b_n}\right)\sum_{i=1}^{M}p_i\left(\frac{\eta+\xi_i}{\eta}\right)^{N_\mathrm{d}} I_i + o\left(\frac{1}{\Gamma^{N_\mathrm{d}}}\right) \quad (20b)$$

with

$$I_i = \sum_{j\in\mathcal{B}_i}\frac{1}{2\pi}\int_0^{\phi_{i,j}}\left(\frac{4\sin^2(\theta+\psi_{i,j})}{w_{i,j}}\right)^{N_\mathrm{d}} d\theta. \quad (21)$$

Proof: Equations (20a) and (20b) follow from the power series expansion of $P_{\mathrm{e;ISIC}}(\Gamma)$ and $P_{\mathrm{e;NSNC}}(\Gamma)$ in terms of $1/\Gamma$ near $\Gamma \to \infty$. □

IV. SNR Penalties

This section first defines the SNR penalty and then quantifies the asymptotic SNR penalty for both asymptotically small and large SNR. Comparisons between several types of systems are considered. For a few specific cases, the exact SNR penalty is also provided.

A. Definition of SNR Penalty

The SNR penalty, $\beta(\Gamma)$, of system Y with respect to a reference system X is defined implicitly as[7]

$$P_{e;\mathrm{Y}}(\Gamma) = P_{e;\mathrm{X}}(\beta(\Gamma)^{-1}\Gamma) \quad (22)$$

where we have assumed that system Y has performance inferior to that of system X (i.e., $P_{e;\mathrm{X}}(\Gamma) \le P_{e;\mathrm{Y}}(\Gamma), \forall\Gamma$). In general, it can be shown that the SEP is monotonically decreasing in Γ and is typically log-concave [43]. Note that the SNR penalty is a function of the target SEP and, therefore, is written explicitly as a function of the average SNR. The derivation of the required SNR for a given target SEP is an inverse problem, which also arises in deriving the bit or symbol error outage [44]–[47] and in determining configuration thresholds for adaptive communication systems [48]–[54]. In general, a closed-form expression for $\beta(\Gamma)$ is difficult to obtain, if at all possible. This paper will focus on four SNR penalties related to two classes of systems, as depicted in Fig. 1. These penalties are implicitly defined as

$$P_{\mathrm{e;ISIC}}(\Gamma) = P^{\mathrm{MRC}}_{\mathrm{e;ISIC}}(\beta(\Gamma)^{-1}\Gamma) \quad (23)$$

$$P_{\mathrm{e;NSNC}}(\Gamma;\eta) = P_{\mathrm{e;ISIC}}(\breve{\beta}(\Gamma)^{-1}\Gamma) \quad (24)$$

$$P_{\mathrm{e;NSNC}}(\Gamma;\eta) = P^{\mathrm{MRC}}_{\mathrm{e;NSNC}}(\tilde{\beta}(\Gamma)^{-1}\Gamma;\eta) \quad (25)$$

$$P_{\mathrm{e;NSNC}}(\Gamma;\eta_1) = P_{\mathrm{e;NSNC}}(\mathring{\beta}(\Gamma)^{-1}\Gamma;\eta_2), \quad \eta_2 > \eta_1. \quad (26)$$

The first penalty (23), concerning only ideal systems, is the penalty of a system employing SSD with respect to one employing MRC. The second penalty (24) is a comparison between non-ideal systems and ideal systems employing the same combining architecture. The third penalty (25), analogous to the first, but for non-ideal systems, is the penalty of a system employing SSD with respect to one employing MRC. Finally, the fourth penalty (26), a generalization of the second, is a comparison between two non-ideal systems with different amounts of energy devoted to channel estimation. Essentially, we are considering two different types of comparisons: 1) comparisons between different combining architectures, with or without channel estimation [i.e., (23) and (25)]; and 2) comparisons between systems with different estimation accuracies [i.e., (24) and (26)], but with the same combining architecture.

TABLE I
SNR Penalties Under Consideration

Penalty	System X	System Y
β	Ideal MRC	Ideal SSD
$\tilde{\beta}$	Non-ideal MRC	Non-ideal SSD
$\breve{\beta}$	Ideal SSD	Non-ideal SSD
$\mathring{\beta}$	Non-ideal SSD ($\eta_2 > \eta_1$)	Non-ideal SSD (η_1)
$\check{\beta}$	Ideal MRC	Non-Ideal SSD

Channel estimation techniques typically utilize resources that may be devoted to data transmission. If the total energy devoted to the data and pilot symbols is constrained, then increasing $N_\mathrm{p}\varepsilon$ leads to greater energy for channel estimation while lowering the energy for data transmission; the two changes have opposite effects on the system performance.[8] To isolate the impact of channel estimation energy on system performance, we focus on the SNR penalty for the case where varying the channel estimation capability does not influence the energy devoted to the data symbols.

Remark: Alternatively, it is also possible to define the SNR penalty with respect to system Y, as given by

$$P_{e;\mathrm{Y}}(\beta'(\Gamma)\Gamma) = P_{e;\mathrm{X}}(\Gamma). \quad (27)$$

If $\beta(\Gamma)$ and $\beta'(\Gamma)$ are independent of Γ, then the definitions in (22) and (27) are equivalent. However, in the case where there is a dependence on Γ, the following two relations hold:

$$\beta(\Gamma) = \beta'\left(\beta(\Gamma)^{-1}\Gamma\right) \quad (28)$$

$$\beta'(\Gamma) = \beta\left(\beta'(\Gamma)\Gamma\right). \quad (29)$$

Throughout the paper, we will restrict our attention to the first definition as given in (22).

In general, the exact SNR penalty (22) is a function of the target SNR; hence, closed-form expressions are difficult, if at all possible, to obtain. To alleviate these issues, we define the asymptotic penalty. The basic methodology is to define a relationship between two asymptotic SEP expressions. In fact, when both asymptotic expressions have the same order, the asymptotic penalty will simply be a scale factor that makes the two expressions touch at the asymptote.

In the following sections, we derive asymptotic SNR penalties, for both small and large SNR, for comparisons between a variety of systems.

B. Comparisons Between Combining Architectures

This section quantifies the asymptotic penalties between different combining architectures for ISIC and NSNC systems. Specifically, Theorem 1 considers the comparison of SSD to

[7]The notation $f(x)^{-1}$ denotes the function $g(x) = 1/f(x)$.

[8]The problem of allocating the energy between the data and pilot symbols has been addressed in the context of adaptive diversity communications (see, e.g., [41]) and in mobile radio systems (see, e.g., [55]).

MRC for NSNC systems. Similarly, Theorem 2 considers the comparison of SSD to MRC for ISIC systems.

Theorem 1: The asymptotic SNR penalties, for small and large SNR, of SSD with respect to MRC for NSNC systems are given, respectively, by

$$\tilde{\beta}_{\mathrm{a}} = \left[\frac{\kappa(\mathbf{1})}{\kappa(\boldsymbol{b})}\right] \tag{30a}$$

$$\tilde{\beta}_{\mathrm{A}} = \left[\prod_n \frac{1}{b_n}\right]^{1/N_{\mathrm{d}}}. \tag{30b}$$

Proof: From Lemma 1, the asymptotic expansion of $P_{\mathrm{e;NSNC}}(\Gamma)$ for small SNR for SSD and MRC is given, respectively, by

$$P_{\mathrm{e;a,NSNC}}(\Gamma) = \frac{\bar{\phi}}{2\pi} - \eta^{1/2}\frac{\bar{\omega}}{2}\kappa(\boldsymbol{b})\Gamma + o(\Gamma) \tag{31}$$

$$P_{\mathrm{e;a,NSNC}}^{\mathrm{MRC}}(\Gamma) = \frac{\bar{\phi}}{2\pi} - \eta^{1/2}\frac{\bar{\omega}}{2}\kappa(\mathbf{1})\Gamma + o(\Gamma). \tag{32}$$

Since these two functions have the same order, with a change of scale of Γ, they will touch asymptotically. From (22), the asymptotic penalty is given by the value of $\tilde{\beta}_{\mathrm{a}}$ such that

$$P_{\mathrm{e;a,NSNC}}(\Gamma) = P_{\mathrm{e;a,NSNC}}^{\mathrm{MRC}}(\tilde{\beta}_{\mathrm{a}}^{-1}\Gamma). \tag{33}$$

Substituting (31) and (32) into (33) gives (30a), which proves the first half of Theorem 1.

From Lemma 2, the asymptotic expansion of $P_{\mathrm{e;NSNC}}(\Gamma)$ for large SNR for SSD and MRC is given, respectively, by

$$P_{\mathrm{e;A,NSNC}}(\Gamma) = \frac{1}{\Gamma^{N_{\mathrm{d}}}}\left(\prod_{n=1}^{N_{\mathrm{d}}}\frac{1}{b_n}\right)\sum_{i=1}^{M} p_i \left(\frac{\eta+\xi_i}{\eta}\right)^{N_{\mathrm{d}}} I_i + o\left(\frac{1}{\Gamma^{N_{\mathrm{d}}}}\right) \tag{34}$$

$$P_{\mathrm{e;A,NSNC}}^{\mathrm{MRC}}(\Gamma) = \frac{1}{\Gamma^{N_{\mathrm{d}}}}\sum_{i=1}^{M} p_i \left(\frac{\eta+\xi_i}{\eta}\right)^{N_{\mathrm{d}}} I_i + o\left(\frac{1}{\Gamma^{N_{\mathrm{d}}}}\right). \tag{35}$$

Again, with a change of scale these two functions will touch asymptotically. From (22) the asymptotic penalty is then given by the value of β_{A} such that

$$P_{\mathrm{e;A,NSNC}}(\Gamma) = P_{\mathrm{e;A,NSNC}}^{\mathrm{MRC}}({\beta_{\mathrm{A}}}^{-1}\Gamma). \tag{36}$$

Substituting (34) and (35) into (36) gives (30b), which proves the second half of Theorem 1. □

Remark: Since $P_{\mathrm{e;NSNC}}^{\mathrm{MRC}}(\Gamma) \leq P_{\mathrm{e;NSNC}}(\Gamma)$, a change in scale of Γ in $P_{\mathrm{e;NSNC}}^{\mathrm{MRC}}(\cdot)$, i.e., $P_{\mathrm{e;NSNC}}^{\mathrm{MRC}}(\tilde{\beta}_{\mathrm{a}}^{-1}\Gamma)$, is like moving $P_{\mathrm{e;NSNC}}^{\mathrm{MRC}}(\Gamma)$ to the right by $10\log_{10}\tilde{\beta}_{\mathrm{a}}$ when plotted on a decibel scale for Γ. The value of $\tilde{\beta}_{\mathrm{a}}$ is the shift that causes the asymptotes to touch.

Theorem 2: The asymptotic SNR penalties, for small and large SNR, of SSD with respect to MRC for ISIC systems are given, respectively, by

$$\beta_{\mathrm{a}} = \left[\frac{\kappa(\mathbf{1})}{\kappa(\boldsymbol{b})}\right]^2 \tag{37a}$$

$$\beta_{\mathrm{A}} = \left[\prod_n \frac{1}{b_n}\right]^{1/N_{\mathrm{d}}}. \tag{37b}$$

Proof: The proof is similar to Theorem 1 using the ISIC expressions from Lemma 1 (12a) and Lemma 2 (20a). □

Remark: The results of Theorem 2 are in complete agreement with those of [23] given for the specific case of H-S/MRC of M-PSK signal constellations, and [37] given for H-S/MRC of arbitrary two-dimensional signal constellations. The results given here unify those in [23], [37] and extend the analysis to the case of SSD with non-ideal channel estimation.

Remark: Theorems 1 and 2 compare combining architectures for the case of NSNC and ISIC systems, respectively. Note that the asymptotic penalties for large SNR in these two cases are equal ($\beta_{\mathrm{A}} = \tilde{\beta}_{\mathrm{A}}$). In fact, for large SNR, an NSNC system has performance approaching that of an ISIC system, and thus, the asymptotic penalties become equal.

C. Comparisons Between Channel Estimation Accuracies

This section quantifies the asymptotic penalties between systems with different amounts of energy devoted to channel estimation for SSD systems. Specifically, Theorems 3 and 4 consider the penalty of an NSNC system with respect to an ISIC system, for asymptotically small and large SNR, respectively. Similarly, Theorem 5 considers the penalty of one NSNC system with respect to another that has more energy devoted to channel estimation, for asymptotically small and large SNR.

Theorem 3: The asymptotic SNR penalty of an NSNC system with respect to an ISIC system for small SNR is unbounded, i.e.,

$$\breve{\beta}_{\mathrm{a}} \to \infty. \tag{38}$$

Proof: Letting $\beta_0 = \breve{\beta}_{\mathrm{a}}^{-1}$, we seek a β_0 such that

$$P_{\mathrm{e;a,NSNC}}(\Gamma) = P_{\mathrm{e;a,ISIC}}(\beta_0\Gamma). \tag{39}$$

Now, let $\beta_0^{1/2} \triangleq \eta^{1/2}\Gamma^{1/2} + o(\Gamma^{1/2})$. From Lemma 1, we have

$$\begin{aligned} P_{\mathrm{e;a,ISIC}}(\beta_0\Gamma) &= \frac{\bar{\phi}}{2\pi} - \frac{\bar{\omega}}{2}\kappa(\boldsymbol{b})\beta_0^{1/2}\Gamma^{1/2} + o\left(\beta_0^{1/2}\Gamma^{1/2}\right) \\ &= \frac{\bar{\phi}}{2\pi} - \eta^{1/2}\frac{\bar{\omega}}{2}\kappa(\boldsymbol{b})\Gamma - \frac{\bar{\omega}}{2}\kappa(\boldsymbol{b})o(\Gamma^{1/2})\Gamma^{1/2} \\ &\quad + o\left(\left(\eta^{1/2}\Gamma^{1/2} + o(\Gamma^{1/2})\right)\Gamma^{1/2}\right). \end{aligned}$$

It can be shown that $-\frac{\bar{\omega}}{2}\kappa(\boldsymbol{b})o(\Gamma^{1/2})\Gamma^{1/2} \in o(\Gamma)$ and $o\left(\left(\eta^{1/2}\Gamma^{1/2} + o(\Gamma^{1/2})\right)\Gamma^{1/2}\right) \in o(\Gamma)$. Thus, we have

$$P_{\mathrm{e;a,ISIC}}(\beta_0\Gamma) = \frac{\bar{\phi}}{2\pi} - \frac{\bar{\omega}}{2}\kappa(\boldsymbol{b})\eta^{1/2}\Gamma + o(\Gamma) = P_{\mathrm{e;a,NSNC}}(\Gamma)$$

where the last equality follows from Lemma 1. Hence, β_0 is a unique solution for a given $\Gamma > 0$. Now by taking the limit of β_0, for $\Gamma \to 0$, we have

$$\lim_{\Gamma\to 0}\beta_0 = \left(\lim_{\Gamma\to 0}\eta^{1/2}\Gamma^{1/2} + o(\Gamma^{1/2})\right)^2 = 0.$$

This implies that $\breve{\beta}_{\mathrm{a}} \to \infty$. □

Theorem 4: The asymptotic SNR penalty of an NSNC system with respect to an ISIC system for large SNR is given by

$$\breve{\beta}_{\mathrm{A}} = \left(\sum_{n=0}^{N_{\mathrm{d}}} c_n \eta^{-n} \right)^{1/N_{\mathrm{d}}} \tag{40}$$

where $c_n = \binom{N_{\mathrm{d}}}{n} \frac{\sum_{i=1}^{M} p_i I_i \xi_i^n}{\sum_{i=1}^{M} p_i I_i}$ and I_i is given by (21).

Proof: From Lemma 2, the asymptotic expansion of $P_{\mathrm{e;ISIC}}(\Gamma)$ for ISIC and NSNC is given by (20a) and (20b), respectively. The asymptotic penalty is given by the value of $\breve{\beta}_{\mathrm{A}}$ such that

$$P_{\mathrm{e;A,NSNC}}(\Gamma) = P_{\mathrm{e;A,ISIC}}(\breve{\beta}_{\mathrm{A}}^{-1}\Gamma). \tag{41}$$

Using (20a) and (20b) in (41) yields [30]

$$\breve{\beta}_{\mathrm{A}} = \left(\frac{\sum_{i=1}^{M} p_i \left(\frac{\eta+\xi_i}{\eta}\right)^{N_{\mathrm{d}}} I_i}{\sum_{i=1}^{M} p_i I_i} \right)^{1/N_{\mathrm{d}}}. \tag{42}$$

Performing the binomial expansion and rearranging terms gives

$$\breve{\beta}_{\mathrm{A}} = \frac{1}{\eta} \left(\sum_{n=0}^{N_{\mathrm{d}}} \eta^{N_{\mathrm{d}}-n} \binom{N_{\mathrm{d}}}{n} \frac{\sum_{i=1}^{M} p_i I_i \xi_i^n}{\sum_{i=1}^{M} p_i I_i} \right)^{1/N_{\mathrm{d}}}. \tag{43}$$

□

Remark: Theorems 3 and 4 show that, when comparing an NSNC system and an ISIC system with the same combining architecture, the asymptotic penalty is the same regardless of the selection vector $\boldsymbol{a}$.

Theorem 5 deals with comparisons between two NSNC SSD systems with different amounts of energy devoted to channel estimation.

Theorem 5: The asymptotic SNR penalties, for small and large SNR, of one NSNC SSD system (η_1) with respect to another NSNC SSD system with greater channel estimation energy $(\eta_2 > \eta_1)$ are given, respectively, by

$$\mathring{\beta}_{\mathrm{a}} = \left[\frac{\eta_2}{\eta_1}\right]^{1/2} \tag{44a}$$

$$\mathring{\beta}_{\mathrm{A}} = \left(\frac{\sum_{n=0}^{N_{\mathrm{d}}} c_n \eta_1^{-n}}{\sum_{n=0}^{N_{\mathrm{d}}} c_n \eta_2^{-n}} \right)^{1/N_{\mathrm{d}}}. \tag{44b}$$

Proof: The proof follows from the asymptotic expressions given in Lemma 1 and Lemma 2. □

It is interesting to note that the asymptotic penalties between two ISIC systems [see (37a) and (37b)] and two NSNC systems [see (30a) and (30b)] have no dependence on the signal constellation. However, the asymptotically large SNR penalty between an ISIC system and an NSNC system (40) or two NSNC systems with different estimation energies (44b) depends on the particular signal constellation.

D. Exact SNR Penalties

Under certain circumstances, it is possible to characterize the exact SNR penalty between NSNC and ISIC systems. In the following, we consider the case of M-PSK signaling. For M-PSK, the exact SNR penalty of an NSNC system with respect to an ISIC system is given by

$$\breve{\beta}(\Gamma) = \frac{1}{\eta\Gamma} + \breve{\beta}_{\mathrm{A}} \tag{45}$$

where $\breve{\beta}_{\mathrm{A}} = (\eta+1)/\eta$. This can be shown by finding a function $\breve{\beta}(\Gamma)$ such that

$$P_{\mathrm{e;NSNC}}^{M-\mathrm{PSK}}(\Gamma) = P_{\mathrm{e;ISIC}}^{M-\mathrm{PSK}}(\breve{\beta}(\Gamma)^{-1}\Gamma). \tag{46}$$

The aforementioned relation is satisfied when the terms in the products of the SEP expressions (given by (10) with (6) for NSNC, and (10) with (5) for ISIC) are equal, i.e.,

$$\frac{\sin^2(\theta)}{b_n \frac{\eta c_{\mathrm{MPSK}}\Gamma^2}{1+(\eta+1)\Gamma} + \sin^2(\theta)} = \frac{\sin^2(\theta)}{b_n c_{\mathrm{MPSK}} \breve{\beta}(\Gamma)^{-1}\Gamma + \sin^2(\theta)}.$$

Canceling terms and solving for $\breve{\beta}(\Gamma)$ gives the expression in (45). From (45), we can see that

$$\breve{\beta}(\Gamma) > \breve{\beta}_{\mathrm{A}} \tag{47a}$$

$$\lim_{\Gamma\to 0+} \breve{\beta}(\Gamma) = \breve{\beta}a = +\infty \tag{47b}$$

$$\lim_{\Gamma\to +\infty} \breve{\beta}(\Gamma) = \breve{\beta}_{\mathrm{A}}. \tag{47c}$$

Similarly, for M-PSK, the exact SNR penalty of one NSNC system (η_1) with respect to another NSNC system with greater channel estimation energy $(\eta_2 > \eta_1)$ is given by

$$\mathring{\beta}(\Gamma) = -\frac{\eta_2+1}{2}\Gamma + \sqrt{\left(\frac{\eta_2+1}{2}\Gamma\right)^2 + \eta_2\frac{\eta_1+1}{\eta_1}\Gamma + \frac{\eta_2}{\eta_1}}. \tag{48}$$

This can be shown by determining a function $\mathring{\beta}(\Gamma)$ such that

$$P_{\mathrm{e;NSNC}}^{M-\mathrm{PSK}}(\Gamma;\eta_1) = P_{\mathrm{e;NSNC}}^{M-\mathrm{PSK}}(\mathring{\beta}(\Gamma)^{-1}\Gamma;\eta_2). \tag{49}$$

The aforementioned relation is satisfied when the terms in the products of the SEP expressions (given by (10) with (6) for $\eta = \eta_1$ and $\eta = \eta_2$) are equal, i.e.,

$$\frac{\sin^2(\theta)}{b_n \frac{\eta_1 c_{\mathrm{MPSK}}\Gamma^2}{1+(\eta_1+1)\Gamma} + \sin^2(\theta)} = \frac{\sin^2(\theta)}{b_n \frac{\eta_2 c_{\mathrm{MPSK}}\mathring{\beta}(\Gamma)^{-2}\Gamma^2}{1+(\eta_2+1)\mathring{\beta}(\Gamma)^{-1}\Gamma} + \sin^2(\theta)}.$$

Canceling terms and solving for $\mathring{\beta}(\Gamma)$ gives the expression in (48), from which we make the following observations:

$$\lim_{\Gamma\to 0+} \mathring{\beta}(\Gamma) = \mathring{\beta}_{\mathrm{a}} \tag{50a}$$

$$\lim_{\Gamma\to +\infty} \mathring{\beta}(\Gamma) = \mathring{\beta}_{\mathrm{A}} = \frac{\eta_2}{\eta_1}\frac{\eta_1+1}{\eta_2+1} \tag{50b}$$

$$\mathring{\beta}_{\mathrm{A}} \le \mathring{\beta}(\Gamma) \le \mathring{\beta}_{\mathrm{a}}, \quad \text{for} \quad 1 \le \sqrt{\eta_1\eta_2} \tag{50c}$$

$$\mathring{\beta}_{\mathrm{a}} \le \mathring{\beta}(\Gamma) \le \mathring{\beta}_{\mathrm{A}}, \quad \text{for} \quad 1 > \sqrt{\eta_1\eta_2}. \tag{50d}$$

That is, the exact SNR penalty is lower and upper bounded by the asymptotic SNR penalties and approaches these limits for small and large SNR.

When the exact SNR penalty is difficult to obtain, asymptotic expressions for the SNR penalties are useful. However, it is also important to develop ways to assess and relate the performance of ISIC and NSNC systems for a specific SNR. The next section provides bounds and approximations to alleviate these difficulties.

V. Bounds and Approximations

In this section, bounds on the SNR penalty are given by using the SEP of an MRC system to upper and lower bound the SEP of ISIC and NSNC. Approximate expressions for the SNR penalties are also given to compare NSNC and ISIC, as well as NSNC with η_1 and NSNC with $\eta_2 > \eta_1$. These expressions can be used to approximate the SEP of one SSD system in terms of another SSD system.

A. Comparisons Between Combining Architectures

We now derive upper and lower bounds on the SNR penalty of SSD with respect to MRC for both NSNC and ISIC systems. This enables us to bound and approximate the SEP of one system in terms of another.

Theorem 6: The SNR penalty of SSD with respect to MRC for NSNC systems is lower and upper bounded by $\tilde{\beta}_{\rm L} \leq \tilde{\beta}(\Gamma) \leq \tilde{\beta}_{\rm U}$, where $\tilde{\beta}_{\rm L}$ and $\tilde{\beta}_{\rm U}$ are defined as

$$\tilde{\beta}_{\rm L} \triangleq \left[\frac{N_{\rm d}}{\sum_n b_n}\right]^{1/2} \tag{51a}$$

$$\tilde{\beta}_{\rm U} \triangleq \left[\prod_n \frac{1}{b_n}\right]^{1/N_{\rm d}}. \tag{51b}$$

Proof: The proof is given in Appendix B. □

Theorem 7: The SNR penalty of SSD with respect to MRC for ISIC systems is lower and upper bounded by $\beta_{\rm L} \leq \beta(\Gamma) \leq \beta_{\rm U}$, where $\beta_{\rm L}$ and $\beta_{\rm U}$ are defined as

$$\beta_{\rm L} \triangleq \frac{N_{\rm d}}{\sum_n b_n} = \tilde{\beta}_{\rm L}^2 \tag{52a}$$

$$\beta_{\rm U} \triangleq \left[\prod_n \frac{1}{b_n}\right]^{1/N_{\rm d}} = \tilde{\beta}_{\rm U}. \tag{52b}$$

Proof: The proof follows from similar arguments to those in the proof of Theorem 6. □

Remark: The results of Theorem 7 are in agreement with those of [23], given for the specific case of H-S/MRC of M-PSK, and [37], given for the case of H-S/MRC of arbitrary two-dimensional signal constellations. The aforementioned results unify those in [23], [37] and extend the analysis to the case of SSD with non-ideal channel estimation.

Equivalently, Theorems 6 and 7 can be used to bound the SEP of NSNC and ISIC SSD systems, respectively:

$$P_{\rm e;NSNC}^{\rm MRC}(\tilde{\beta}_{\rm L}^{-1}\Gamma;\eta) \leq P_{\rm e;NSNC}(\Gamma;\eta) \leq P_{\rm e;NSNC}^{\rm MRC}(\tilde{\beta}_{\rm U}^{-1}\Gamma;\eta) \tag{53}$$

$$P_{\rm e;ISIC}^{\rm MRC}(\beta_{\rm L}^{-1}\Gamma) \leq P_{\rm e;ISIC}(\Gamma) \leq P_{\rm e;ISIC}^{\rm MRC}(\beta_{\rm U}^{-1}\Gamma). \tag{54}$$

The equivalence, in both cases, is due to the definitions of $\tilde{\beta}$ and β, and to the fact that $P_{\rm e;NSNC}(\Gamma;\eta)$ and $P_{\rm e;ISIC}(\Gamma)$ are *strict monotonically decreasing* functions of Γ. Equation (53) states that the SEP of an NSNC system employing SSD can be lower and upper bounded by the SEP of an NSNC system employing MRC operating at $\tilde{\beta}_{\rm L}^{-1}\Gamma$ and $\tilde{\beta}_{\rm U}^{-1}\Gamma$, respectively.

Similarly, (54) states that the SEP of an ISIC system employing SSD can be lower and upper bounded by the SEP of an ISIC system employing MRC operating at $\beta_{\rm L}^{-1}\Gamma$ and $\beta_{\rm U}^{-1}\Gamma$, respectively.

Using Theorems 6 and 7, the SNR penalty of SSD with respect to MRC for NSNC and ISIC systems, respectively, can be approximated by taking the geometric mean of the upper and lower bounds as

$$\tilde{\beta}_{\rm approx} \approx (\tilde{\beta}_{\rm L}\tilde{\beta}_{\rm U})^{1/2} \tag{55}$$

$$\beta_{\rm approx} \approx (\beta_{\rm L}\beta_{\rm U})^{1/2}. \tag{56}$$

Here, the geometric mean of the upper and lower bounds, on a linear scale, is used to obtain the arithmetic mean of the bounds on a decibel scale. Then, the performance of ISIC and NSNC systems employing SSD can be approximated as

$$P_{\rm e;NSNC}(\Gamma;\eta) \approx P_{\rm e;NSNC}^{\rm MRC}\left(\tilde{\beta}_{\rm approx}^{-1}\Gamma;\eta\right) \tag{57}$$

$$P_{\rm e;ISIC}(\Gamma) \approx P_{\rm e;ISIC}^{\rm MRC}\left(\beta_{\rm approx}^{-1}\Gamma\right). \tag{58}$$

B. Comparisons Between Channel Estimation Accuracies

We now derive approximations of the SNR penalty for NSNC systems with respect to ISIC systems, with the same combining architecture. Similarly, we also consider the SNR penalty for comparisons between NSNC systems. This enables us to approximate the SEP of one system in terms of another.

It is difficult to formulate good upper and lower bounds for the SNR penalty between ISIC and NSNC systems, as well as the penalty between two NSNC systems with different amounts of energy devoted to estimation. For instance, note that $\breve{\beta}(\Gamma)$ tends toward infinity for small Γ. This makes a formulation like the ones in (53) and (54) impractical. Instead, we take the approach of approximating the SNR penalty using the notion of conditional SNR penalties.

Definition 1: The conditional SNR penalty of system Y with respect to system X, $\beta_i(\Gamma)$, is defined as the SNR penalty based on the conditional SEP given that symbol s_i is transmitted:

$$P_{e|s_i,{\rm Y}}(\Gamma) = P_{e|s_i,{\rm X}}(\beta_i(\Gamma)^{-1}\Gamma). \tag{59}$$

Theorem 8: The conditional SNR penalty of an NSNC system with respect to an ISIC system is given by

$$\breve{\beta}_i(\Gamma) = \frac{1}{\eta\,\Gamma} + \frac{\eta+\xi_i}{\eta}. \tag{60}$$

Proof: The conditional SNR penalty is the expression $\breve{\beta}_i(\Gamma)$ that satisfies

$$P_{\rm e|s_i,NSNC}(\Gamma;\eta) = P_{\rm e|s_i,ISIC}(\breve{\beta}_i(\Gamma)^{-1}\Gamma) \tag{61}$$

where, from (3)–(6)

$$P_{\mathrm{e}|s_i,\mathrm{ISIC}}(\Gamma) = \sum_{j\in\mathcal{B}_i} I_{N_\mathrm{d}}\left(\boldsymbol{b}\frac{w_{i,j}}{4}\Gamma, \phi_{i,j}, \psi_{i,j}\right) \quad (62)$$

$$P_{\mathrm{e}|s_i,\mathrm{NSNC}}(\Gamma;\eta) = \sum_{j\in\mathcal{B}_i} I_{N_\mathrm{d}}\left(\boldsymbol{b}\frac{w_{i,j}}{4}\frac{\eta\Gamma^2}{1+(\eta+\xi_i)\Gamma}, \phi_{i,j}, \psi_{i,j}\right) \quad (63)$$

are the conditional SEPs for ISIC and NSNC, respectively. An explicit expression for $\breve{\beta}_i(\Gamma)$ can be determined by using (62) and (63) in (61), along with the expression for $I_{N_\mathrm{d}}(\cdot,\cdot,\cdot)$ given in (4). Equating similar terms gives

$$\frac{\sin^2(\theta+\psi_{i,j})}{b_n\frac{w_{i,j}}{4}\frac{\eta\Gamma^2}{1+(\eta+\xi_i)\Gamma} + \sin^2(\theta+\psi_{i,j})} = \frac{\sin^2(\theta+\psi_{i,j})}{b_n\frac{w_{i,j}}{4}\breve{\beta}_i(\Gamma)^{-1}\Gamma + \sin^2(\theta+\psi_{i,j})}. \quad (64)$$

Canceling terms and solving for $\breve{\beta}_i(\Gamma)$ gives (60). □

Using Theorem 8, the SNR penalty of an NSNC system with respect to an ISIC system, $\breve{\beta}(\Gamma)$, can be approximated as

$$\breve{\beta}(\Gamma) \approx \breve{\beta}_{\mathrm{approx}}(\Gamma) \triangleq \sum_{i=1}^{M} p_i\breve{\beta}_i(\Gamma) = \frac{1}{\eta\Gamma} + \frac{\eta+1}{\eta} \quad (65)$$

where $\breve{\beta}_i(\Gamma)$ is given in (60) and the second equality follows from the fact that $\sum_{i=1}^{M} p_i\xi_i = 1$.

Theorem 9: The conditional SNR penalty of one NSNC SSD system (η_1) with respect to another NSNC SSD system with greater channel estimation energy $(\eta_2 > \eta_1)$ is given by

$$\mathring{\beta}_i(\Gamma) = -\frac{\eta_2+\xi_i}{2}\Gamma + \sqrt{\left(\frac{\eta_2+\xi_i}{2}\Gamma\right)^2 + \eta_2\frac{\eta_1+\xi_i}{\eta_1}\Gamma + \frac{\eta_2}{\eta_1}}. \quad (66)$$

Proof: The conditional SNR penalty is the expression $\beta_i(\Gamma)$ that satisfies

$$P_{\mathrm{e}|s_i,\mathrm{NSNC}}(\Gamma;\eta_1) = P_{\mathrm{e}|s_i,\mathrm{NSNC}}(\mathring{\beta}_i(\Gamma)^{-1}\Gamma;\eta_2), \quad \eta_2 > \eta_1 \quad (67)$$

where $P_{\mathrm{e}|s_i,\mathrm{NSNC}}(\Gamma;\eta)$ is the conditional SEP as given by (63). In this case, it is possible to find an explicit expression for $\beta_i(\Gamma)$ by using (63) in(67) and setting similar terms equal to each other, yielding the following quadratic equation:

$$\frac{\eta_2\mathring{\beta}_i(\Gamma)^{-2}}{1+(\eta_2+\xi_i)\mathring{\beta}_i(\Gamma)^{-1}\Gamma} = \frac{\eta_1}{1+(\eta_1+\xi_i)\Gamma}. \quad (68)$$

Taking the positive root gives the expression in (66). □

The following observations about the conditional SNR penalty (66) are made, but the proofs are omitted for brevity:

$$\mathring{\beta}_{a,i} \triangleq \lim_{\Gamma\to 0}\mathring{\beta}_i(\Gamma) = \left[\frac{\eta_2}{\eta_1}\right]^{1/2} \quad (69a)$$

$$\mathring{\beta}_{A,i} \triangleq \lim_{\Gamma\to\infty}\mathring{\beta}_i(\Gamma) = \frac{\eta_2}{\eta_1}\frac{\eta_1+\xi_i}{\eta_2+\xi_i} \quad (69b)$$

$$\mathring{\beta}_{A,i} \le \mathring{\beta}_i(\Gamma) \le \mathring{\beta}_{a,i}, \quad \text{for} \quad \xi_i \le \sqrt{\eta_1\eta_2} \quad (69c)$$

$$\mathring{\beta}_{a,i} \le \mathring{\beta}_i(\Gamma) \le \mathring{\beta}_{A,i}, \quad \text{for} \quad \xi_i > \sqrt{\eta_1\eta_2}. \quad (69d)$$

Using Theorem 9, the SNR penalty of one NSNC system (η_1) with respect to another NSNC system $(\eta_2 > \eta_1)$ can be approximated by

$$\mathring{\beta}(\Gamma) \approx \mathring{\beta}_{\mathrm{approx}}(\Gamma) \triangleq \sum_{i=1}^{M} p_i\mathring{\beta}_i(\Gamma) \quad (70)$$

where $\mathring{\beta}_i(\Gamma)$ is given in (66).

Now, using (65) and (70), the SEP of NSNC systems can be approximated as

$$P_{\mathrm{e;NSNC}}(\Gamma;\eta) \approx P_{\mathrm{e;ISIC}}(\breve{\beta}_{\mathrm{approx}}(\Gamma)^{-1}\Gamma) \quad (71)$$

$$P_{\mathrm{e;NSNC}}(\Gamma;\eta_1) \approx P_{\mathrm{e;NSNC}}(\mathring{\beta}_{\mathrm{approx}}(\Gamma)^{-1}\Gamma;\eta_2). \quad (72)$$

Equation (71) states that the SEP of an NSNC system with η estimation energy operating at an SNR Γ is approximately equal to the SEP of an ISIC system operating at a SNR of $\breve{\beta}_{\mathrm{approx}}(\Gamma)^{-1}\Gamma$. Similarly, (72) indicates that the SEP of an NSNC system with η_1 estimation energy operating at an SNR Γ is approximately equal to the SEP of an NSNC system with η_2 estimation energy at an SNR of $\mathring{\beta}_{\mathrm{approx}}(\Gamma)^{-1}\Gamma$.

C. Combination of SNR Penalties

An ISIC MRC system provides the best possible performance and thus can be used as a reference system. The comparison of any other system with respect to this reference can then be obtained via a combination of SNR penalties. In particular, it can be shown that the SNR penalty of NSNC SSD with respect to ISIC MRC, defined as

$$P_{\mathrm{e;NSNC}}(\Gamma;\eta) = P_{\mathrm{e;ISIC}}^{\mathrm{MRC}}(\breve{\beta}(\Gamma)^{-1}\Gamma) \quad (73)$$

is given by

$$\breve{\beta}(\Gamma) = \beta(\breve{\beta}(\Gamma)^{-1}\Gamma)\breve{\beta}(\Gamma) \quad (74a)$$

$$= \breve{\beta}(\tilde{\beta}(\Gamma)^{-1}\Gamma)\tilde{\beta}(\Gamma). \quad (74b)$$

Note that these two expressions are equivalent, but arise from considering different penalties in the process of formulating the overall comparison. The expression in (74a) first uses the penalty of NSNC SSD with respect to ISIC SSD, and then with respect to ISIC MRC. On the other hand, the expression in (74b) first uses the penalty of NSNC SSD with respect to NSNC MRC, and then with respect to ISIC MRC.

In general, since the exact expressions for all the penalties involved in the aforementioned expressions are not known, we can use the previously developed bounds to approximate $\breve{\beta}(\Gamma)$. Specifically, starting from (74a), we approximate $\beta(\cdot)$ with the geometric mean of its lower and upper bounds, as in (58), and $\breve{\beta}(\cdot)$ with the approximation in (65), resulting in[9]

$$\breve{\beta}(\Gamma) \approx \breve{\beta}_{\mathrm{approx}}(\Gamma) \triangleq \sqrt{\beta_\mathrm{L}\beta_\mathrm{U}}\breve{\beta}_{\mathrm{approx}}(\Gamma). \quad (75)$$

D. Approximation Accuracy

To evaluate the efficacy of the approximations, we have developed, we examine the SNR difference (in dB) between these approximations and the true penalty determined numerically. In particular, we will consider metrics of the following form:

$$\Delta\beta = \max_{\Gamma\le\Gamma^{\mathrm{th}}}\left|\beta_{(\mathrm{dB})}(\Gamma) - \beta_{\mathrm{approx\,(dB)}}(\Gamma)\right| \quad (76)$$

[9]Equation (74a) was chosen over (74b) because the approximation for β is better than that for $\tilde{\beta}$, since the upper and lower bounds are closer.

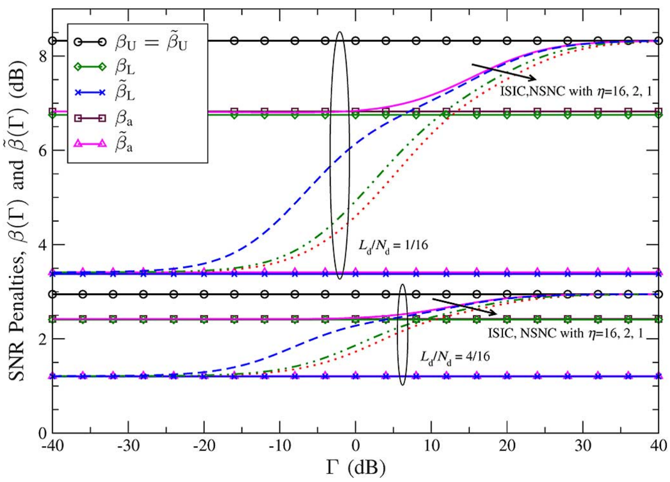

Fig. 3. SNR penalty for 16-QAM, 16-branch SSD for various values of L_d and η. Upper and lower bounds are also shown.

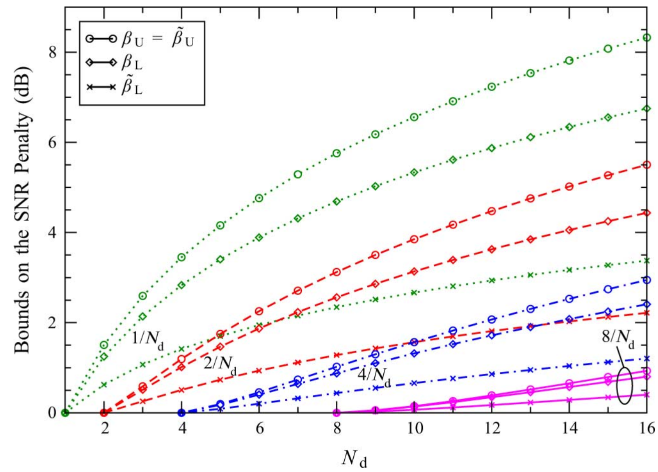

Fig. 4. Lower and upper bounds for the SNR penalty between two ideal systems (β) and two non-ideal systems ($\tilde{\beta}$).

for an SNR penalty $\beta(\cdot)$ and its approximation $\beta_{\text{approx}}(\cdot)$. Here, Γ^{th} is chosen such that $P_e^{\text{th}} = P_{e;Y}(\Gamma^{\text{th}})$, for an SEP threshold P_e^{th} which indicates the smallest SEP of interest. The metric in (76) gives the maximum difference (in dB) between the approximation and the true performance for any SEP greater than P_e^{th}. This metric measures the overall accuracy of an approximation by considering its accuracy for all SEPs greater than P_e^{th} or, equivalently, all SNRs less than Γ^{th}.

VI. Discussion

The methodology and expressions developed in this paper are applicable for different combining architectures, varying degrees of channel estimation energies, and arbitrary two-dimensional signal constellations. We now demonstrate how these expressions facilitate system design using specific examples. In particular, we consider 16-QAM systems to illustrate the behavior of the SNR penalty, bounds, and the accuracy of the approximations derived in the previous sections. First, we discuss the two penalties for the comparison of systems with different combining architectures (β and $\tilde{\beta}$). Second, we examine the two penalties for the comparison of systems with different estimation accuracies ($\breve{\beta}$ and $\mathring{\beta}$). Third, we discuss the comparison between ideal MRC and non-ideal SSD, which can be viewed as a combination of the previous two types of penalties. In all cases, the exact penalties are computed by numerically evaluating the SEP expressions in conjunction with a numerical root-finding operation. Specifically, we consider H-S/MRC systems where the receiver combines the signals from the L_d antennas with the largest estimated channel magnitude out of N_d available antennas.[10] For this selection policy

$$\boldsymbol{a} = [\underbrace{1\ 1\ \cdots\ 1}_{L_d \text{ terms}}\ 0\ 0\ \cdots\ 0]^T$$

which yields $b_n = 1$, for $1 \le n \le L_d$, and $b_n = L_d/n$, for $L_d < n \le N_d$.

[10]Recall that NSNC systems utilize the estimates of the channel gains during both the selection and combining processes.

A. Combining Architecture

Figure 3 shows the SNR penalty between SSD and MRC systems for both ISIC $\beta(\Gamma)$ and NSNC $\tilde{\beta}(\Gamma)$ with $N_d = 16$ branches. The figure also shows the upper and lower bounds on these penalties as well as the large and small asymptotes. Note that $\beta_U = \tilde{\beta}_U = \beta_A = \tilde{\beta}_A$, i.e., the SNR penalties between two ISIC systems $\beta(\Gamma)$ and two NSNC systems $\tilde{\beta}(\Gamma)$ share the same upper bound and this bound is asymptotically tight. It can be seen that the difference between β_L and β_a is typically in the second or third significant digit as reported in [23] for the specific case of M-PSK ISIC systems. Thus, little is lost in using the lower bound to assess the asymptotic performance. The difference between the values of $\tilde{\beta}_L$ and $\tilde{\beta}_a$ in dB is half that of β_L and β_a, since $\tilde{\beta}_L = \beta_L^{1/2}$ and $\tilde{\beta}_a = {\beta_a}^{1/2}$. From this figure, we also see that for larger values of the estimation accuracy, η, the SNR penalty $\tilde{\beta}(\Gamma)$ approaches the ideal SNR penalty $\beta(\Gamma)$ more quickly . However, the upper and lower bounds, as well as the large and small asymptotes, remain independent of η.

We see in Fig. 3 that the difference between the upper and lower bounds depends on the specific value of L_d. To obtain further insights, Fig. 4 shows β_U, $\tilde{\beta}_U$, β_L, and $\tilde{\beta}_L$, as a function of N_d for $L_d = 1, 2, 4, 8$. It is clear from Figs. 3 and 4 that there is a large difference in the range of β and $\tilde{\beta}$. Examining the upper and lower bounds for both cases reveals that this difference is $\beta_L/2$ (in dB). Since the bounds are tight, this implies that the SNR penalty as a function of Γ varies more in non-ideal systems. However, the worst case SNR penalty is the same for both cases, since they share the same upper bound. For the case of β, the maximum difference between the upper and lower bounds is 1.57 dB, while for $\tilde{\beta}$ it is 4.95 dB.

B. Channel Estimation Accuracy

Figure 5 shows the SNR penalty of an NSNC system with respect to an ISIC system (24), along with the approximation (65), for various values of η and L_d. From these plots, it can be observed that the approximation is quite accurate for a range of SNRs. These SNRs, those less than about 20 dB, are reasonable for practical systems. Also note that the approximation becomes increasingly more accurate as the estimation energy η

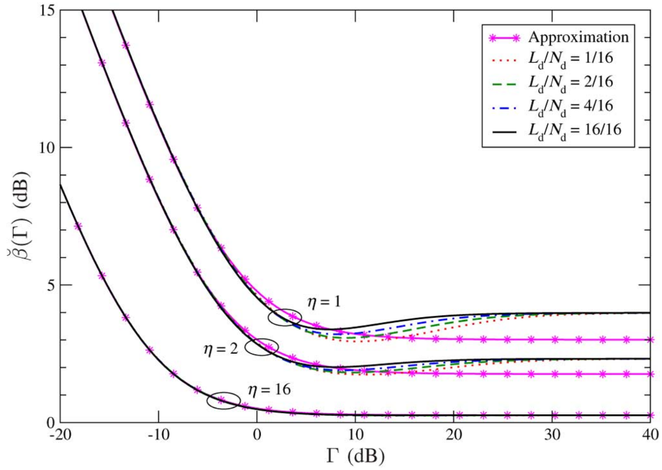

Fig. 5. SNR penalty $\breve{\beta}(\Gamma)$ between NSNC and ISIC for 16-QAM, 16-branch SSD systems.

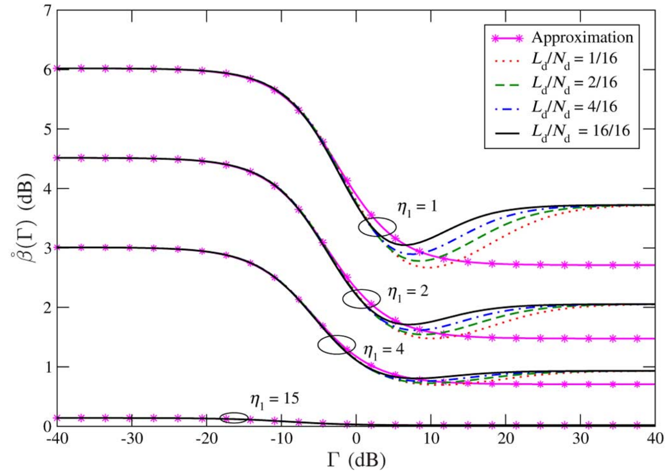

Fig. 7. SNR penalty $\mathring{\beta}(\Gamma)$ between two NSNC systems for 16-QAM, 16-branch SSD ($\eta_2 = 16$).

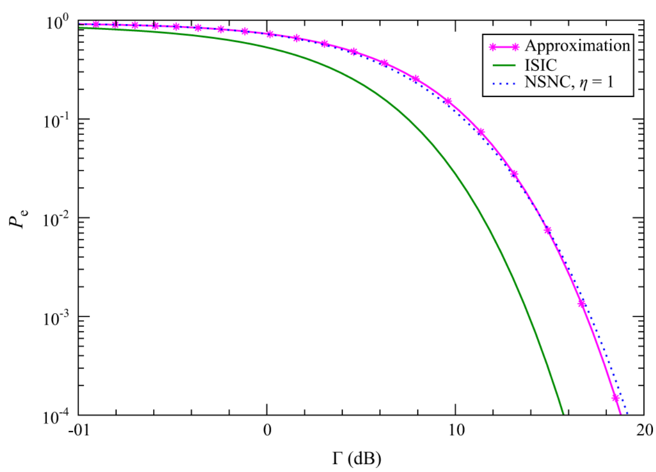

Fig. 6. SEP for a 16-QAM, $L_d/N_d = 1/16$ SSD system and the SEP approximation for NSNC with $\eta = 1$ using an ISIC system [based on $\breve{\beta}_{\text{approx}}(\Gamma)$ in (65)].

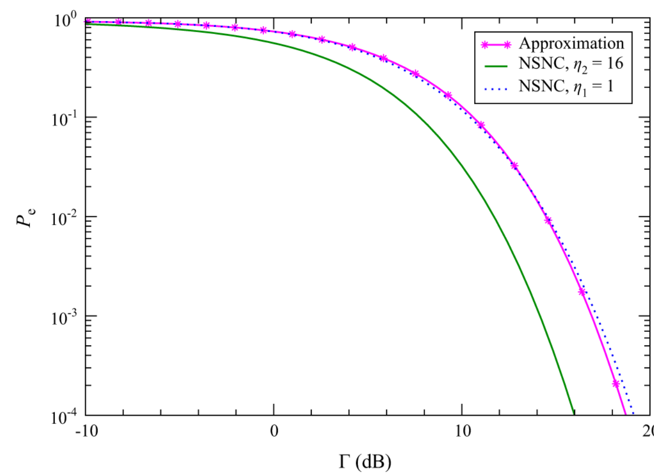

Fig. 8. SEP for a 16-QAM, $L_d/N_d = 1/16$ SSD system and the SEP approximation for NSNC with $\eta = 1$ using an NSNC system with $\eta_2 = 16$ [based on $\mathring{\beta}_{\text{approx}}(\Gamma)$ in (70)].

increases. To better quantify this effect, Table II lists the approximation accuracy $\Delta\breve{\beta}$ for various η and L_d (top number in each table entry). All values in Table II are based on $P_e^{th} = 10^{-6}$, but a similar table can be produced for any P_e^{th} of interest. These values are conservative since typical values of P_e for uncoded systems, such as 10^{-2} or 10^{-3}, are greater than P_e^{th}. These data indicate that the performance gaps are approximately equal over the range of L_d and, as suggested by Fig. 5, the gap decreases quickly as η increases. The table also indicates that the performance gap is at worst about 0.6 dB for a 16-QAM, 16-branch system with $\eta \geq 1$. To further illustrate the application of the approximation, Fig. 6 shows the SEP of $L_d/N_d = 1/16$ ISIC and NSNC systems with $\eta = 1$, along with an approximation to the NSNC performance curve. The approximation is formed as indicated by (71). From the figure, it can be noted that the approximation is accurate for all SNRs of interest.

Similarly, Fig. 7 shows the SNR penalty of one NSNC system with respect to an NSNC system (26) with $\eta_2 = 16$, along with the approximation (70), for various values of η_1 and L_d. Again, it is clear that the approximation is accurate for a range of SNRs that are reasonable for practical systems. As for the case above, the SNR penalty quickly decreases and the approximation becomes more accurate as η_1 approaches η_2. To better quantify the difference between the true SNR penalty and the approximation, Table II lists the estimation accuracy $\Delta\mathring{\beta}$ for various values of L_d and η (middle number in each table entry). The data indicate that the performance gap is at most about 0.65 dB for a 16-QAM, 16-branch system with $\eta_1 \geq 1$. For increasing values of η_1, the table shows that the performance gap decreases quickly. To further illustrate the application of the approximation, Fig. 8 shows the SEP of two $L_d/N_d = 1/16$ NSNC systems: one with $\eta_2 = 16$ and another with $\eta_1 = 1$. The approximation to the $\eta_1 = 1$ system, formed as indicated by (72), is also shown. Also in this case, it can be noted from the figure that the approximation is accurate for all SNRs of interest.

C. Combination of SNR Penalties

The SNR penalty of an NSNC system employing SSD with respect to an ISIC system employing MRC (73), along with the approximation (75), is shown in Fig. 9 for various values of η and L_d. This figure shows the combined effect of channel estimation accuracy, as well as combining architecture. To assess the aggregate effect, we combine the approximations for the SNR penalty of ideal SSD with respect to ideal MRC (58), as well as the penalty of non-ideal SSD with respect to ideal SSD (65). The approximation accuracy improves as the number of combined branches $L_{\rm d}$, or the estimation accuracy η increases. This behavior is further verified by the data given in Table II. The table lists the approximation accuracy $\Delta\breve{\beta}$ for various values of $L_{\rm d}$ and η (bottom number in each table entry). The data indicate that the performance gap is at worst about 1.01 dB for SEPs greater than 10^{-6}.

VII. Conclusion

This paper defines the SNR penalty between two systems with different combining architectures and varying degrees of channel estimation energy, for arbitrary two-dimensional signal constellations. According to this definition, we derive the asymptotic SNR penalties, for both small and large SNR, between a variety of SSD systems. We also derive upper and lower bounds, as well as approximations, on the SNR penalty.

We demonstrate that the SNR penalty of SSD with respect to MRC has the same upper bound and asymptotic behavior (large SNR) for both ISIC and NSNC systems. On the other hand, the lower bounds and asymptotic behaviors (small SNR) of these penalties differ by a power of two. Thus, NSNC systems suffer a penalty which is at most equal to that of ISIC systems, but the range of the penalty for NSNC is larger. These behaviors illustrate the dual role of channel estimation in practical diversity systems.

The derived SNR penalties enable simple and accurate performance assessment of one diversity system in terms of another. Specifically, it is shown that the approximations are a fraction of a decibel away from the exact SNR penalty that require extensive numerical evaluation. The notion of SNR penalty allows system designers to assess sensitivity to channel estimation energy, combining architecture, and signal constellation, which in turn facilitates making decisions during the design of wireless systems.

Appendix A
SEP Expansion for Asymptotically Small SNR

In this appendix, the expansion of the SEP for NSNC at asymptotically small SNR is derived for two cases.

Lemma 3: For asymptotically small Γ, the expansion of

$$p(\Gamma) = \frac{1}{2\pi}\int_{\psi}^{\phi}\prod_{n=1}^{N_{\rm d}}\left[\frac{\sin^2\theta}{b_n f(\Gamma)+\sin^2\theta}\right]d\theta,\quad 0<\psi<\phi<\pi$$

where $f(\Gamma)=\frac{a\Gamma^2}{1+c\Gamma}$, for finite a and c, is given by

$$p(\Gamma)\approx\frac{\phi-\psi}{2\pi}+o(\Gamma).$$

Proof: Let

$$g(\Gamma)=\frac{\phi-\psi}{2\pi}-p(\Gamma)$$

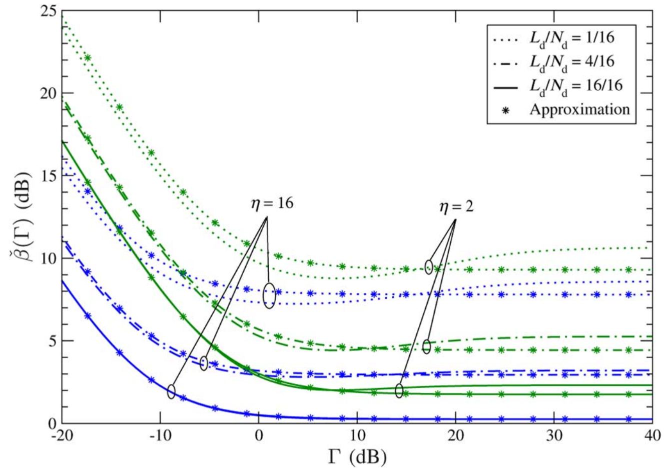

Fig. 9. SNR penalty $\breve{\beta}(\Gamma)$ between SSD NSNC and ideal MRC for 16-QAM, 16-branch systems.

$$=\frac{1}{2\pi}\int_{\psi}^{\phi}\left\{1-\prod_{n=1}^{N_{\rm d}}\left[\frac{\sin^2\theta}{b_n f(\Gamma)+\sin^2\theta}\right]\right\}d\theta. \quad (77)$$

Let $B=\max_n\{b_n\}$, then

$$g(\Gamma)\le\frac{1}{2\pi}\int_{\psi}^{\phi}\left\{1-\left[\frac{\sin^2\theta}{Bf(\Gamma)+\sin^2\theta}\right]^{N_{\rm d}}\right\}d\theta$$
$$=\frac{1}{2\pi}\int_{\psi}^{\phi}\left\{1-\left[1-\frac{Bf(\Gamma)}{Bf(\Gamma)+\sin^2\theta}\right]^{N_{\rm d}}\right\}d\theta. \quad (78)$$

It can be shown by induction that $1-(1-q)^{N_{\rm d}}\le N_{\rm d}q, \forall N_{\rm d}\ge 1$ and $q\le 1$. Using this fact, (78) becomes

$$g(\Gamma)\le\frac{1}{2\pi}\int_{\psi}^{\phi}\frac{N_{\rm d}Bf(\Gamma)}{Bf(\Gamma)+\sin^2\theta}d\theta$$
$$\le\frac{1}{2\pi}\int_{\psi}^{\phi}\frac{N_{\rm d}Bf(\Gamma)}{Bf(\Gamma)+\sin^2(\tilde{\delta}(\psi,\phi))}d\theta$$

where $\tilde{\delta}(\psi,\phi)=\arg\min_{\theta\in[\psi,\phi]}\sin^2\theta$. This implies

$$\frac{1}{\Gamma}g(\Gamma)\le\frac{1}{2\pi}\frac{N_{\rm d}B\,(\phi-\psi)\,\frac{a\Gamma}{1+c\Gamma}}{B\frac{a\Gamma^2}{1+c\Gamma}+\sin^2\left(\tilde{\delta}(\psi,\phi)\right)}.$$

Note that $\sin^2(\tilde{\delta}(\psi,\phi))>0$ since $0<\psi<\phi<\pi$, and hence

$$\limsup_{\Gamma\to 0}\frac{1}{\Gamma}g(\Gamma)\le 0. \quad (79)$$

On the other hand, it is clear from the definition of $g(\cdot)$ that $g(\Gamma)\ge 0$. Thus, in conjunction with (79), we have

$$\lim_{\Gamma\to 0}\frac{1}{\Gamma}g(\Gamma)=0.$$

Thus, $g(\Gamma)=o(\Gamma)$. This result, combined with (77), completes the proof of Lemma 3. □

TABLE II
APPROXIMATION ACCURACY IN DECIBELS. $\Delta\breve{\beta}$ (TOP), AND $\Delta\mathring{\beta}$ (MIDDLE), AND $\Delta\check{\beta}$ (BOTTOM) ARE SHOWN FOR $P_{\mathrm{e}}^{\mathrm{th}} = 10^{-6}$

η_1	$L_{\mathrm{d}}/N_{\mathrm{d}}$ 1/16	2/16	4/16	8/16	12/16	14/16	15/16	16/16
1	0.57203	0.58172	0.59384	0.60240	0.60376	0.60367	0.60358	0.60353
	0.62623	0.63517	0.64616	0.65350	0.65436	0.65416	0.65406	0.65399
	1.01496	0.78404	0.62306	0.60569	0.60427	0.60377	0.60361	0.60353
2	0.25510	0.26165	0.27000	0.27616	0.27731	0.27731	0.27727	0.27724
	0.29573	0.30170	0.30918	0.31445	0.31526	0.31519	0.31514	0.31510
	0.86663	0.64903	0.41225	0.27946	0.27782	0.27741	0.27730	0.27724
4	0.11122	0.10815	0.10416	0.09981	0.09850	0.09815	0.09806	0.09801
	0.09107	0.09394	0.09765	0.10049	0.10107	0.10110	0.10109	0.10108
	0.78509	0.56789	0.33463	0.15379	0.10531	0.09923	0.09827	0.09801
6	0.07734	0.07586	0.07403	0.07180	0.07048	0.07041	0.07039	0.07038
	0.03962	0.03811	0.03826	0.03983	0.04020	0.04021	0.04021	0.04021
	0.76031	0.54101	0.30583	0.12585	0.07733	0.07149	0.07060	0.07038
8	0.05948	0.05864	0.05767	0.05666	0.05546	0.05545	0.05544	0.05544
	0.02418	0.02346	0.02249	0.02146	0.02093	0.02087	0.02085	0.02084
	0.74938	0.52774	0.29110	0.11033	0.06225	0.05652	0.05565	0.05544
10	0.04856	0.04813	0.04733	0.04643	0.04581	0.04582	0.04582	0.04583
	0.01468	0.01432	0.01381	0.01325	0.01295	0.01292	0.01291	0.01290
	0.74401	0.52090	0.28246	0.10040	0.05256	0.04688	0.04603	0.04583
12	0.04106	0.04077	0.04039	0.03953	0.03905	0.03908	0.03909	0.03909
	0.00825	0.00805	0.00780	0.00751	0.00736	0.00734	0.00733	0.00733
	0.74105	0.51689	0.27688	0.09350	0.04578	0.04014	0.03930	0.03909
14	0.03559	0.03539	0.03515	0.03477	0.03405	0.03409	0.03410	0.03411
	0.00356	0.00348	0.00339	0.00327	0.00321	0.00320	0.00320	0.00320
	0.73923	0.51432	0.27289	0.08862	0.04076	0.03515	0.03431	0.03411

Lemma 4: For asymptotically small Γ, the expansion of

$$p(\Gamma) = \frac{1}{2\pi}\int_0^{\phi}\prod_{n=1}^{N_{\mathrm{d}}}\left[\frac{\sin^2\theta}{b_n f(\Gamma)+\sin^2\theta}\right]d\theta, \quad 0<\phi<\pi$$

where $f(\Gamma) = \frac{a\Gamma^2}{1+c\Gamma}$, for finite a and c, is given by

$$p(\Gamma) \approx \frac{\phi}{2\pi} - a^{1/2}\kappa(\boldsymbol{b})\Gamma + o(\Gamma).$$

Proof: Let

$$g(\Gamma) = \frac{\phi}{2\pi} - p(\Gamma). \tag{80}$$

Define a sufficiently small ϵ, such that $\epsilon \geq 0$ and $\tilde{\epsilon} = \epsilon/(a^{1/2}\kappa(\boldsymbol{b})) \in [0,1)$. The continuity of $\theta/\sin\theta$, around $\theta = 0$, implies that there exists $\delta(\epsilon)$ such that

$$\frac{1}{1+\tilde{\epsilon}} \leq \frac{\sin\theta}{\theta} \leq \frac{1}{1-\tilde{\epsilon}} \tag{81}$$

whenever $\theta \leq \delta(\epsilon)$. For such $\delta(\epsilon)$, $g(\Gamma)$ can be rewritten in terms of two separate integrals as

$$g(\Gamma) = I_1(\Gamma,\epsilon) + I_2(\Gamma,\epsilon) \tag{82}$$

where

$$I_1(\Gamma,\epsilon) \triangleq \frac{1}{2\pi}\int_0^{\delta(\epsilon)}\left\{1-\prod_{n=1}^{N_{\mathrm{d}}}\left[\frac{\sin^2\theta}{b_n f(\Gamma)+\sin^2\theta}\right]\right\}d\theta \tag{83}$$

$$I_2(\Gamma,\epsilon) \triangleq \frac{1}{2\pi}\int_{\delta(\epsilon)}^{\phi}\left\{1-\prod_{n=1}^{N_{\mathrm{d}}}\left[\frac{\sin^2\theta}{b_n f(\Gamma)+\sin^2\theta}\right]\right\}d\theta. \tag{84}$$

First, as a consequence of Lemma 3, we have

$$I_2(\Gamma,\epsilon) \approx o(\Gamma). \tag{85}$$

Now, we will show that for any $\epsilon \in \left[0, a^{1/2}\kappa(\boldsymbol{b})\right)$

$$\limsup_{\Gamma\to 0}\left|\frac{1}{\Gamma}I_1(\Gamma,\epsilon) - a^{1/2}\kappa(\boldsymbol{b})\right| \leq \epsilon. \tag{86}$$

From (83)

$$I_1(\Gamma,\epsilon) = \frac{1}{2\pi}\int_0^{\delta(\epsilon)}\left\{1-\prod_{n=1}^{N_{\mathrm{d}}}\left[1-\frac{b_n f(\Gamma)}{b_n f(\Gamma)+\sin^2\theta\frac{\theta^2}{\theta^2}}\right]\right\}d\theta.$$

Using (81)

$$\begin{aligned} I_1(\Gamma,\epsilon) &\leq \frac{1}{2\pi}\int_0^{\delta(\epsilon)}\left\{1-\prod_{n=1}^{N_{\mathrm{d}}}\left[1-\frac{b_n f(\Gamma)}{b_n f(\Gamma)+\frac{\theta^2}{(1+\tilde{\epsilon})^2}}\right]\right\}d\theta \\ &= \frac{1}{2\pi}\int_0^{(\delta(\epsilon)/(1+\tilde{\epsilon}))(1/f(\Gamma))^{1/2}}\left\{1-\prod_{n=1}^{N_{\mathrm{d}}}\left[\frac{u^2}{b_n+u^2}\right]\right\} \\ &\qquad \cdot [f(\Gamma)]^{1/2}(1+\tilde{\epsilon})du \end{aligned} \tag{87}$$

where, in the second equation, we have used the change of variables $u = (\theta/(1+\tilde{\epsilon}))(1/f(\Gamma))^{1/2}$. Taking the $\limsup$ on both sides of (87) gives

$$\begin{aligned} &\limsup_{\Gamma\to 0}\frac{1}{\Gamma}I_1(\Gamma,\epsilon) \\ &\quad\leq \frac{1}{2\pi}\int_0^{\infty}\left\{1-\prod_{n=1}^{N_{\mathrm{d}}}\left[\frac{u^2}{b_n+u^2}\right]\right\}a^{1/2}(1+\tilde{\epsilon})du \\ &\quad= a^{1/2}\kappa(\boldsymbol{b})(1+\tilde{\epsilon}) \end{aligned}$$

and therefore

$$\limsup_{\Gamma\to 0}\left[\frac{1}{\Gamma}I_1(\Gamma,\epsilon) - a^{1/2}\kappa(\boldsymbol{b})\right] \leq \epsilon. \tag{88}$$

A similar argument using the right inequality of (81) yields

$$\liminf_{\Gamma\to 0}\left[\frac{1}{\Gamma}I_1(\Gamma,\epsilon)-a^{1/2}\kappa(\boldsymbol{b})\right]\geq -\epsilon. \tag{89}$$

Equations (88) and (89) imply that

$$\limsup_{\Gamma\to 0}\left|\frac{1}{\Gamma}I_1(\Gamma,\epsilon)-a^{1/2}\kappa(\boldsymbol{b})\right|\leq \epsilon \tag{90}$$

which completes the proof of (86).

Using (82) and (85) in conjunction with (90) gives

$$\limsup_{\Gamma\to 0}\left|\frac{1}{\Gamma}g(\Gamma)-a^{1/2}\kappa(\boldsymbol{b})\right|\leq \epsilon.$$

The above is true for all $\epsilon\in\left[0,a^{1/2}\kappa(\boldsymbol{b})\right)$, and thus

$$\lim_{\Gamma\to 0}\frac{1}{\Gamma}g(\Gamma)=a^{1/2}\kappa(\boldsymbol{b}).$$

This, together with (82), implies that

$$p(\Gamma)\approx\frac{\phi}{2\pi}-a^{1/2}\kappa(\boldsymbol{b})\Gamma+o(\Gamma)$$

which completes the proof of Lemma 4. □

Appendix B
Proof of the SEP Bounds for NSNC

In this appendix, a proof is given for the SEP bounds for comparing NSNC systems employing SSD with respect to NSNC systems employing MRC.

Proof (Lower Bound): For each i, j, Γ, and $\theta\in[0,\phi_{i,j}]$, let

$$x_n=\frac{b_n\Gamma\frac{\eta}{\frac{1}{\Gamma}+\eta+\xi_i}\frac{w_{i,j}}{4}+\sin^2(\theta+\psi_{i,j})}{\sin^2(\theta+\psi_{i,j})}.$$

Since $x_n\geq 0$, [23, Th. 3] implies that, for any probability vector $\boldsymbol{p}$

$$\sum_n p_n\left[\frac{b_n\Gamma\frac{\eta}{\frac{1}{\Gamma}+\eta+\xi_i}\frac{w_{i,j}}{4}+\sin^2(\theta+\psi_{i,j})}{\sin^2(\theta+\psi_{i,j})}\right] \geq\prod_n\left[\frac{b_n\Gamma\frac{\eta}{\frac{1}{\Gamma}+\eta+\xi_i}\frac{w_{i,j}}{4}+\sin^2(\theta+\psi_{i,j})}{\sin^2(\theta+\psi_{i,j})}\right]^{p_n}.$$

Using $p_n=1/N_{\mathrm{d}}$ and applying Lemma 5 gives

$$\left[\frac{\tilde{\beta}_{\mathrm{L}}^{-1}\Gamma\frac{\eta}{\frac{1}{\tilde{\beta}_{\mathrm{L}}^{-1}\Gamma}+\eta+\xi_i}\frac{w_{i,j}}{4}+\sin^2(\theta+\psi_{i,j})}{\sin^2(\theta+\psi_{i,j})}\right]^{N_{\mathrm{d}}} \geq\prod_n\left[\frac{b_n\Gamma\frac{\eta}{\frac{1}{\Gamma}+\eta+\xi_i}\frac{w_{i,j}}{4}+\sin^2(\theta+\psi_{i,j})}{\sin^2(\theta+\psi_{i,j})}\right]$$

where $\tilde{\beta}_{\mathrm{L}}^{-1}=\left(\sum_n\frac{b_n}{N_{\mathrm{d}}}\right)^{1/2}$. Integrating the inverse of both sides over θ and scaling by $1/(2\pi)$ gives

$$I_{N_{\mathrm{d}}}^{\mathrm{MRC}}(\boldsymbol{\zeta}^{(i,j)}(\tilde{\beta}_{\mathrm{L}}^{-1}\Gamma),\phi_{i,j},\psi_{i,j}) \leq I_{N_{\mathrm{d}}}(\boldsymbol{\zeta}^{(i,j)}(\Gamma),\phi_{i,j},\psi_{i,j})\quad\forall i,j$$

where $\zeta_n^{(i,j)}(\Gamma)$ is given by (6), and therefore

$$\sum_{j\in\mathcal{B}_i}I_{N_{\mathrm{d}}}^{\mathrm{MRC}}(\boldsymbol{\zeta}^{(i,j)}(\tilde{\beta}_{\mathrm{L}}^{-1}\Gamma),\phi_{i,j},\psi_{i,j}) \leq\sum_{j\in\mathcal{B}_i}I_{N_{\mathrm{d}}}(\boldsymbol{\zeta}^{(i,j)}(\Gamma),\phi_{i,j},\psi_{i,j})\quad\forall i.$$

Recognizing that (3) with (9) and (3) with (4) are convex combinations of the terms on the left-hand side and right-hand side, respectively, yields

$$P_{\mathrm{e;NSNC}}^{\mathrm{MRC}}(\tilde{\beta}_{\mathrm{L}}^{-1}\Gamma)\leq P_{\mathrm{e;NSNC}}(\Gamma).$$

□

Proof (Upper Bound): Using ESF-Sum Inequality [23, Th. 4], it can be shown for any nonnegative $\boldsymbol{y}$ that

$$\prod_n(y_n+1)\geq\left[\prod_n y_n^{1/N_{\mathrm{d}}}+1\right]^{N_{\mathrm{d}}}. \tag{91}$$

For each i, j, Γ, and $\theta\in[0,\phi_{i,j}]$, let

$$y_n=\frac{b_n\Gamma\frac{\eta}{\frac{1}{\Gamma}+\eta+\xi_i}\frac{w_{i,j}}{4}}{\sin^2(\theta+\psi_{i,j})}.$$

Now, (91) becomes

$$\prod_n\left[\frac{b_n\Gamma\frac{\eta}{\frac{1}{\Gamma}+\eta+\xi_i}\frac{w_{i,j}}{4}+\sin^2(\theta+\psi_{i,j})}{\sin^2(\theta+\psi_{i,j})}\right] \geq\left[\frac{\left(\prod_n b_n\right)^{1/N_{\mathrm{d}}}\Gamma\frac{\eta}{\frac{1}{\Gamma}+\eta+\xi_i}\frac{w_{i,j}}{4}+\sin^2(\theta+\psi_{i,j})}{\sin^2(\theta+\psi_{i,j})}\right]^{N_{\mathrm{d}}}.$$

Application of Lemma 5 to the right-hand side gives

$$\prod_n\left[\frac{b_n\Gamma\frac{\eta}{\frac{1}{\Gamma}+\eta+\xi_i}\frac{w_{i,j}}{4}+\sin^2(\theta+\psi_{i,j})}{\sin^2(\theta+\psi_{i,j})}\right] \geq\left[\frac{\tilde{\beta}_{\mathrm{U}}^{-1}\Gamma\frac{\eta}{\frac{1}{\tilde{\beta}_{\mathrm{U}}^{-1}\Gamma}+\eta+\xi_i}\frac{w_{i,j}}{4}+\sin^2(\theta+\psi_{i,j})}{\sin^2(\theta+\psi_{i,j})}\right]^{N_{\mathrm{d}}}$$

where $\tilde{\beta}_{\mathrm{U}}^{-1}=\left(\prod_n b_n\right)^{1/N_{\mathrm{d}}}$. Integrating the inverse of both sides over θ and scaling by $1/(2\pi)$ gives

$$I_{N_{\mathrm{d}}}(\boldsymbol{\zeta}^{(i,j)}(\Gamma),\phi_{i,j},\psi_{i,j}) \leq I_{N_{\mathrm{d}}}^{\mathrm{MRC}}(\boldsymbol{\zeta}^{(i,j)}(\tilde{\beta}_{\mathrm{L}}^{-1}\Gamma),\phi_{i,j},\psi_{i,j})\quad\forall i,j$$

where $\zeta_n^{(i,j)}(\Gamma)$ is given by (6) and, therefore

$$\sum_{j\in\mathcal{B}_i}I_{N_{\mathrm{d}}}\left(\boldsymbol{\zeta}^{(i,j)}(\Gamma),\phi_{i,j},\psi_{i,j}\right) \leq\sum_{j\in\mathcal{B}_i}I_{N_{\mathrm{d}}}^{\mathrm{MRC}}\left(\boldsymbol{\zeta}^{(i,j)}\left(\tilde{\beta}_{\mathrm{L}}^{-1}\Gamma\right),\phi_{i,j},\psi_{i,j}\right)\quad\forall i.$$

Recognizing that (3) with (4) and (3) with(9) are convex combinations of the terms on the left-hand side and right-hand side, respectively, yields

$$P_{\mathrm{e;NSNC}}(\Gamma) \le P_{\mathrm{e;NSNC}}^{\mathrm{MRC}}(\tilde{\beta}_{\mathrm{U}}^{-1}\Gamma).$$

□

APPENDIX C
BOUNDS ON $\boldsymbol{\zeta}^{(i,j)}(\Gamma)$

As discussed in Section III, the vector $\boldsymbol{\zeta}^{(i,j)}(\Gamma)$ has elements which are a function of the SNR. The following lemma deals with the properties of functions with a form similar to $\zeta_n^{(i,j)}(\Gamma)$ given in (6).

Lemma 5: For any $\alpha \in (0,1]$ and $c \in [0,\infty)$, the function

$$f(\Gamma) \triangleq \frac{\Gamma}{\frac{1}{\Gamma}+c} = \frac{\Gamma^2}{1+c\Gamma}, \quad \Gamma > 0$$

satisfies the following:

$$f(\alpha^{1/2}\Gamma) \ge \alpha f(\Gamma) \ge f(\alpha\Gamma).$$

Proof: Omitted for brevity. □

ACKNOWLEDGMENT

The authors wish to thank N. C. Beaulieu, Y. Shen, L. A. Shepp, and W. Suwansantisuk for valuable discussions and insightful observations, which have greatly improved the quality of the paper. They would also like to thank the editor and the anonymous reviewers for helpful comments.

REFERENCES

[1] M. Z. Win and J. H. Winters, "Analysis of hybrid selection/maximal-ratio combining in Rayleigh fading," *IEEE Trans. Commun.*, vol. 47, no. 12, pp. 1773–1776, Dec. 1999.

[2] J. H. Winters and M. Z. Win, "Hybrid selection/optimum combining," *Proc. IEEE VTS 53rd Conf. Veh. Technol.*, pp. 113–117, 2001.

[3] A. F. Molisch, M. Z. Win, and J. H. Winters, "Reduced-complexity multiple transmit/receive antenna systems," *IEEE Trans. Signal Process*, vol. 51, no. 11, pp. 2729–2738, Nov. 2003.

[4] A. F. Molisch and M. Z. Win, "MIMO systems with antenna selection—An overview," *IEEE Microw. Mag.*, vol. 5, no. 1, pp. 46–56, Mar. 2004.

[5] S. Sanayei and A. Nosratinia, "Antenna selection in MIMO systems," *IEEE Commun. Mag.*, vol. 42, no. 10, pp. 68–73, Oct. 2004.

[6] R. W. Heath and D. J. Love, "Receive antenna selection in MIMO systems using convex optimization," *IEEE Trans. Signal Process.*, vol. 53, no. 8, pp. 3042–3056, Aug. 2005.

[7] A. Dua, K. Medepalli, and A. J. Paulraj, "Receive antenna selection in MIMO systems using convex optimization," *IEEE Trans. Wireless Commun.*, vol. 5, no. 9, pp. 2353–2357, Sep. 2006.

[8] N. B. Mehta and A. Molisch*, Antenna selection in MIMO systems, MIMO antenna technology for wireless*, G. Tsulos, Ed. Boca Raton, FL: CRC Press, 2006.

[9] J. H. Winters, Y.-S. Choi, B.-J. J. Kim, A. F. Molisch, M. Z. Win, and H. Luo, "Method of selecting receive antennas for MIMO systems," U.S. Patent 7 006 810, Feb. 28, 2006.

[10] J. H. Winters, Y.-S. Choi, B.-J. J. Kim, A. F. Molisch, M. Z. Win, and H. Luo, "Method of selecting receive antennas for MIMO systems," U.S. Patent 7 283 798, Oct. 16, 2007.

[11] M. Z. Win and J. H. Winters, "Analysis of hybrid selection/maximal-ratio combining in Rayleigh fading," *IEEE Trans. Commun.*, vol. 47, no. 12, pp. 1773–1776, Dec. 1999.

[12] M. Z. Win and J. H. Winters, "Virtual branch analysis of symbol error probability for hybrid selection/maximal-ratio combining in Rayleigh fading," *IEEE Trans. Commun.*, vol. 49, no. 11, pp. 1926–1934, Nov. 2001.

[13] M. Z. Win, R. K. Mallik, and G. Chrisikos, "Higher order statistics of antenna subset diversity," *IEEE Trans. Wireless Commun.*, vol. 2, no. 5, pp. 871–875, Sep. 2003.

[14] M. Z. Win and J. H. Winters, "Methods and systems for spatial processing," U.S. Patent 6 804 312, Oct. 12, 2004.

[15] M. S. Alouini and M. K. Simon, "Performance of coherent receivers with hybrid SC/MRC over Nakagami—m fading channels," *IEEE Trans. Veh. Technol.*, vol. 48, no. 4, pp. 1155–1164, Jul. 1999.

[16] M. S. Alouini and M. K. Simon, "An MGF-based performance analysis of generalized selection combining over Rayleigh fading channels," *IEEE Trans. Commun.*, vol. 48, no. 3, pp. 401–415, Mar. 2000.

[17] N. Kong and L. B. Milstein, "Average SNR of a generalized diversity selection combining scheme," *IEEE Commun. Lett.*, vol. 3, no. 3, pp. 57–59, Mar. 1999.

[18] X. Zhang and N. C. Beaulieu, "Performance analysis of generalized selection combining in generalized correlated Nakagami—m fading," *IEEE Trans. Commun.*, vol. 54, no. 11, pp. 2103–2112, Nov. 2006.

[19] *Part 11: Wireless LAN Medium Access Control (MAC) and Physical Layer (PHY) Specifications-Amendment 5: Enhancements for Higher Throughput, IEEE Computer Society*, , Oct. 2009.

[20] Technical Specification Group Radio Access Network; Evolved Universal Terrestrial Radio Access (E-UTRA); Multiplexing and Channel Coding, 3rd Generation Partnership Project 3GPP™ TS 36.212 V9.3.0 (2010–09) Oct. 9, 2010 [Online]. Available: http://www.3gpp.org/ftp/specs/html-info/36212.htm

[21] Technical Specification Group Radio Access Network; Evolved Universal Terrestrial Radio Access (E-UTRA); Physical Layer Procedures, 3rd Generation Partnership Project 3GPP™ TS 36.213 V9.3.0 (2010–09) Oct. 9, 2010 [Online]. Available: http://www.3gpp.org/ftp/specs/html-info/36213.htm

[22] *Part 16: Air Interface for Broadband Wireless Access Systems, IEEE Computer Society and IEEE Microwave Theory and Techniques Society*, , May 2009, IEEE Std 802.16-2009.

[23] M. Z. Win, N. C. Beaulieu, L. A. Shepp, B. F. Logan, and J. H. Winters, "On the SNR penalty of MPSK with hybrid selection/maximal ratio combining over IID Rayleigh fading channels," *IEEE Trans. Commun.*, vol. 51, no. 6, pp. 1012–1023, Jun. 2003.

[24] A. Annamalai and C. Tellambura, "Analysis of hybrid selection/maximal-ratio diversity combiners with Gaussian errors," *IEEE Trans. Wireless Commun.*, vol. 1, no. 3, pp. 498–512, Jul. 2002.

[25] X. Wang and J. Wang, "Effect of imperfect channel estimation on transmit diversity in CDMA systems," *IEEE Trans. Veh. Technol.*, vol. 53, no. 5, pp. 1400–1412, Sep. 2004.

[26] W. M. Gifford, M. Z. Win, and M. Chiani, "Diversity with practical channel estimation," *IEEE Trans. Wireless Commun.*, vol. 4, no. 4, pp. 1935–1947, Jul. 2005.

[27] W. M. Gifford, M. Z. Win, and M. Chiani, "Diversity combining with imperfect channel estimates in correlated fading," *IEEE Trans. Aerosp. Electron. Syst.*, vol. 44, no. 3, pp. 852–860, Jul. 2008.

[28] L. Cao and N. C. Beaulieu, "Exact error-rate analysis of diversity 16-QAM with channel estimation error," *IEEE Trans. Commun.*, vol. 52, no. 6, pp. 1019–1029, Jun. 2004.

[29] L. Cao and N. C. Beaulieu, "Closed-form BER results for MRC diversity with channel estimation errors in ricean fading channels," *IEEE Trans. Wireless Commun.*, vol. 4, no. 4, pp. 1440–1447, Jul. 2005.

[30] W. M. Gifford, M. Z. Win, and M. Chiani, "Antenna subset diversity with non-ideal channel estimation," *IEEE Trans. Wireless Commun.*, vol. 7, no. 5, pp. 1527–1539, May 2008.

[31] Y. Chen and N. C. Beaulieu, "SER of selection diversity MFSK with channel estimation errors," *IEEE Trans. Wireless Commun.*, vol. 5, no. 7, pp. 1920–1929, Jul. 2006.

[32] B. Xia and J. Wang, "Effect of channel-estimation error on QAM systems with antenna diversity," *IEEE Trans. Inf. Theory*, vol. 53, no. 3, pp. 481–488, Mar. 2005.

[33] B. Xia and J. Wang, "Analytical study of QAM with interference cancellation for high-speed multicode CDMA," *IEEE Trans. Veh. Technol.*, vol. 54, no. 3, pp. 1070–1080, May 2005.

[34] R. Annavajjala, P. C. Cosman, and L. B. Milstein, "Performance analysis of linear modulation schemes with generalized diversity combining on Rayleigh fading channels with noisy channel estimates," *IEEE Trans. Inf. Theory*, vol. 53, no. 12, pp. 4701–4727, Dec. 2007.

[35] V. Kristem, N. B. Mehta, and A. F. Molisch, "Optimal receive antenna selection in time-varying fading channels with practical training constraints," *IEEE Trans. Commun.*, vol. 58, no. 7, pp. 2023–2034, Jul. 2010.

[36] V. Kristem, N. B. Mehta, and A. F. Molisch, "A novel, balanced, and energy-efficient training method for receive antenna selection," *IEEE Trans. Wireless Commun.*, vol. 9, no. 9, pp. 2742–2753, Sep. 2010.

[37] S. Haghani, N. C. Beaulieu, and M. Z. Win, "Penalty of hybrid diversity for two-dimensional signaling in Rayleigh fading," *IEEE Trans. Commun.*, vol. 52, no. 5, pp. 694–697, May 2004.

[38] S. Haghani, N. C. Beaulieu, and M. Z. Win, "Large penalty of hybrid diversity with uncoded modulation in slow Rayleigh fading," *IEEE Trans. Wireless Commun.*, vol. 5, no. 9, pp. 2363–2368, Sep. 2006.

[39] P. A. Bello and B. D. Nelin, "Predetection diversity combining with selectivity fading channels," *IEEE Trans. Commun. Syst.*, vol. 10, no. 1, pp. 32–42, Mar. 1962.

[40] M. J. Gans, "The effect of Gaussian error in maximal ratio combiners," *IEEE Trans. Commun.*, vol. 19, no. 4, pp. 492–500, Aug. 1971.

[41] L. Toni and A. Conti, "Does fast adaptive modulation always outperform slow adaptive modulation," *IEEE Trans. Wireless Commun.*, vol. 10, no. 5, pp. 1504–1513, May 2011.

[42] A. Conti, W. M. Gifford, M. Z. Win, and M. Chiani, "Optimized simple bounds for diversity systems," *IEEE Trans. Commun.*, vol. 57, no. 9, pp. 2674–2685, Sep. 2009.

[43] A. Conti, D. Panchenko, S. Sidenko, and V. Tralli, "Log-concavity property of the error probability with application to local bounds for wireless communications," *IEEE Trans. Inf. Theory*, vol. 55, no. 6, pp. 2766–2775, Jun. 2009.

[44] P. Mary, M. Dohler, J.-M. Gorce, G. Villemaud, and M. Arndt, "BPSK bit error outage over Nakagami-m fading channels in lognormal shadowing environments," *IEEE Commun. Lett.*, vol. 11, no. 7, pp. 565–567, Jul. 2007.

[45] A. Conti, M. Z. Win, M. Chiani, and J. H. Winters, "Bit error outage for diversity reception in shadowing environment," *IEEE Commun. Lett.*, vol. 7, no. 1, pp. 15–17, Jan. 2003.

[46] P. Mary, M. Dohler, J.-M. Gorce, G. Villemaud, and M. Arndt, "M-ary symbol error outage over Nakagami-m fading channels in shadowing environments," *IEEE Trans. Commun.*, vol. 57, no. 10, pp. 2876–2879, Oct. 2009.

[47] A. Conti, M. Z. Win, and M. Chiani, "On the inverse symbol error probability for diversity reception," *IEEE Trans. Commun.*, vol. 51, no. 5, pp. 753–756, May 2003.

[48] W. T. Webb and R. Steele, "Variable rate QAM for mobile radio," *IEEE Trans. Commun.*, vol. 43, no. 7, pp. 2223–2230, Jul. 1995.

[49] A. J. Goldsmith and S.-G. Chua, "Variable-rate variable-power MQAM for fading channel," *IEEE Trans. Commun.*, vol. 45, no. 10, pp. 1218–1230, Oct. 1997.

[50] X. Qiu and K. Chawla, "On the performance of adaptive modulation in cellular systems," *IEEE Trans. Commun.*, vol. 47, no. 6, pp. 884–895, Jun. 1999.

[51] S. T. Chung and A. J. Goldsmith, "Degree of freedom in adaptive modulation: A unified view," *IEEE Trans. Commun.*, vol. 49, no. 9, pp. 1561–1571, Sep. 2001.

[52] A. Conti, M. Z. Win, and M. Chiani, "Slow adaptive M—QAM with diversity in fast fading and shadowing," *IEEE Trans. Commun.*, vol. 55, no. 5, pp. 895–905, May 2007.

[53] S. Ni, J. S. Blogh, and L. Hanzo, "Adaptive beamforming and adaptive modulation-assisted network performance of multiuser detection-aided FDD and TDD CDMA systems," *IEEE Trans. Veh. Technol.*, vol. 56, no. 4, pp. 1881–1891, Jul. 2007.

[54] H. Bogucka and A. Conti, "Degrees of freedom for energy savings in practical adaptive wireless systems," *IEEE Commun. Mag.*, vol. 49, no. 6, pp. 38–45, Jun. 2011.

[55] M. Chiani, A. Conti, and C. Fontana, "Improved performance in TD-CDMA mobile radio system by optimizing energy partition in channel estimation," *IEEE Trans. Commun.*, vol. 51, no. 3, pp. 352–355, Mar. 2003.

Wesley M. Gifford (S'03–M'10) received the Ph.D. and M.S. degrees in electrical engineering from Massachusetts Institute of Technology in 2010 and 2004, respectively. He received the B.S. degree (*summa cum laude*) from Rensselaer Polytechnic Institute in Computer and Systems Engineering - Computer Science in 2001.

He is currently a research staff member at the IBM Thomas J. Watson Research Center, where he applies mathematical, statistical, and machine learning theories to improve business processes. Prior to joining IBM Research, he was with the Laboratory for Information and Decision Systems (LIDS), MIT, where his work focused on multiple antenna systems, UWB transmission systems, location-aware networks, and measurement and modeling of propagation channels.

Dr. Gifford was a member of the Technical Program Committee (TPC) for the IEEE International Conference on Communications 2011 and the International Conference on Ultra-Wideband 2011. He has also served as a TPC member for the IEEE Global Communications Conference 2009, the IEEE International Conference on Communications 2007, and as a TPC Vice Chair for the IEEE Conference on Ultra Wideband 2006. He received best paper awards at the IEEE Global Communications Conference (2009), at the IEEE First International Conference on Next-Generation Wireless Systems (2006), and at ACM International Wireless Communications and Mobile Computing Conference (2006). He was awarded a Claude E. Shannon Fellowship (2007) and the Frederick C. Hennie III Award (2003) from MIT.

Andrea Conti (S'99–M'01–SM'11) received the Laurea degree (*summa cum laude*) in telecommunications engineering and the Ph.D. degree in electronic engineering and computer science from the University of Bologna, Italy, in 1997 and 2001, respectively.

In 2005, he joined the University of Ferrara, Italy, where he is a Professore Aggregato. He was Researcher with Consorzio Nazionale Interuniversitario per le Telecomunicazioni (CNIT) from 1999 to 2002 and with Istituto di Elettronica e di Ingegneria dell'Informazione e delle Telecomunicazioni, Consiglio Nazionale delle Ricerche (IEIIT/CNR) from 2002 to 2005 at the Research Unit of Bologna. In Summer 2001, he was with the Wireless Systems Research Department at AT&T Research Laboratories. Since 2003, he has been a frequent visitor to the Wireless Communication and Network Sciences Laboratory at the Massachusetts Institute of Technology (MIT), where he presently holds the Research Affiliate appointment. He is a coauthor of *Wireless Sensor and Actuator Networks: Enabling Technologies, Information Processing and Protocol Design* (Elsevier, 2008). His research interests involve theory and experimentation of wireless systems and networks including network localization, adaptive diversity communications, cooperative relaying techniques, interference management, and sensor networks.

Dr. Conti is currently an Editor for the IEEE Communications Letters. He served as an Editor for the IEEE Transactions on Wireless Communications (2003–2009) and Guest-Editor for the EURASIP Journal on Advances in Signal Processing (Special Issue on Wireless Cooperative Networks) in 2008. He is the Technical Program Chair for a number of IEEE conferences. He served as reviewer for IEEE and IET journals and as Technical Program Committee Member for numerous IEEE conferences. He is elected Vice-Chair and Secretary of the IEEE Communications Society's Radio Communications Technical Committee for the terms 2011–2012 and 2009–2010, respectively. He is an elected Fellow of the IET and is an IEEE Distinguished Lecturer for the term 2011–2013.

Marco Chiani (M'94–SM'02–F'11) was born in Rimini, Italy, in April 1964. He received the Dr. Ing. degree (*summa cum laude*) in electronic engineering and the Ph.D. degree in electronic and computer science from the University of Bologna, Italy, in 1989 and 1993, respectively.

He is a Full Professor of Telecommunications and the current Director of the Center for Industrial Research on ICT, University of Bologna. He is a frequent visitor at the Massachusetts Institute of Technology (MIT), Cambridge, where he presently holds a Research Affiliate appointment. He is leading the research unit of the University of Bologna on cognitive radio and UWB (European project EUWB), on Joint Source and Channel Coding for wireless video (European projects Phoenix-FP6 and Optimix-FP7), and is a consultant to the European Space Agency (ESA-ESOC) for the design and evaluation of error correcting codes based on LDPCC for space CCSDS applications. His research interests include wireless communication systems, MIMO systems, wireless multimedia, low-density parity-check codes (LDPCC) and UWB.

Prof. Chiani has chaired, organized sessions, and served on the Technical Program Committees at several IEEE International Conferences. He is the past Chair (2002–2004) of the Radio Communications Committee of the IEEE Communication Society and past Editor of Wireless Communication (2000–2007) for the IEEE TRANSACTIONS ON COMMUNICATIONS.

Moe Z. Win (S'85–M'87–SM'97–F'04) received both the Ph.D. in Electrical Engineering and M.S. in Applied Mathematics as a Presidential Fellow at the University of Southern California (USC) in 1998. He received an M.S. in Electrical Engineering from USC in 1989, and a B.S. (*magna cum laude*) in Electrical Engineering from Texas A&M University in 1987.

He is an Associate Professor at the Massachusetts Institute of Technology (MIT). Prior to joining MIT, he was at AT&T Research Laboratories for five years and at the Jet Propulsion Laboratory for seven years. His research encompasses fundamental theories, algorithm design, and experimentation for a broad range of real-world problems. His current research topics include network localization and navigation, network interference exploitation, intrinsic wireless secrecy, adaptive diversity techniques, and ultra-wide bandwidth systems.

Professor Win is an elected Fellow of the AAAS, the IEEE, and the IET, and was an IEEE Distinguished Lecturer. He was honored with two IEEE Technical Field Awards: the IEEE Kiyo Tomiyasu Award (2011) and the IEEE Eric E. Sumner Award (2006, jointly with R. A. Scholtz). Together with students and colleagues, his papers have received numerous awards including the IEEE Communications Society's Leonard G. Abraham Prize Paper Award (2011), the IEEE Aerospace and Electronic Systems Society's M. Barry Carlton Award (2011), the IEEE Communications Society's Guglielmo Marconi Prize Paper Award (2008), and the IEEE Antennas and Propagation Society's Sergei A. Schelkunoff Transactions Prize Paper Award (2003). Highlights of his international scholarly initiatives are the Copernicus Fellowship (2011), the Royal Academy of Engineering Distinguished Visiting Fellowship (2009), and the Fulbright Fellowship (2004). Other recognitions include the Outstanding Service Award of the IEEE ComSoc Radio Communications Committee (2010), the Laurea Honoris Causa from the University of Ferrara (2008), the Technical Recognition Award of the IEEE ComSoc Radio Communications Committee (2008), the Wireless Educator of the Year Award (2007), and the U.S. Presidential Early Career Award for Scientists and Engineers (2004).

Dr. Win is an elected Member-at-Large on the IEEE Communications Society Board of Governors (2011–2013). He was the chair (2004–2006) and secretary (2002–2004) for the Radio Communications Committee of the IEEE Communications Society. Over the last decade, he has organized and chaired numerous international conferences. He is currently an Editor for IEEE TRANSACTIONS ON WIRELESS COMMUNICATIONS, and served as Area Editor (2003– 2006) and Editor (1998–2006) for the IEEE TRANSACTIONS ON COMMUNICATIONS. He was Guest-Editor for the *Proceedings of the IEEE* (2009) and IEEE JOURNAL ON SELECTED AREAS IN COMMUNICATIONS (2002).